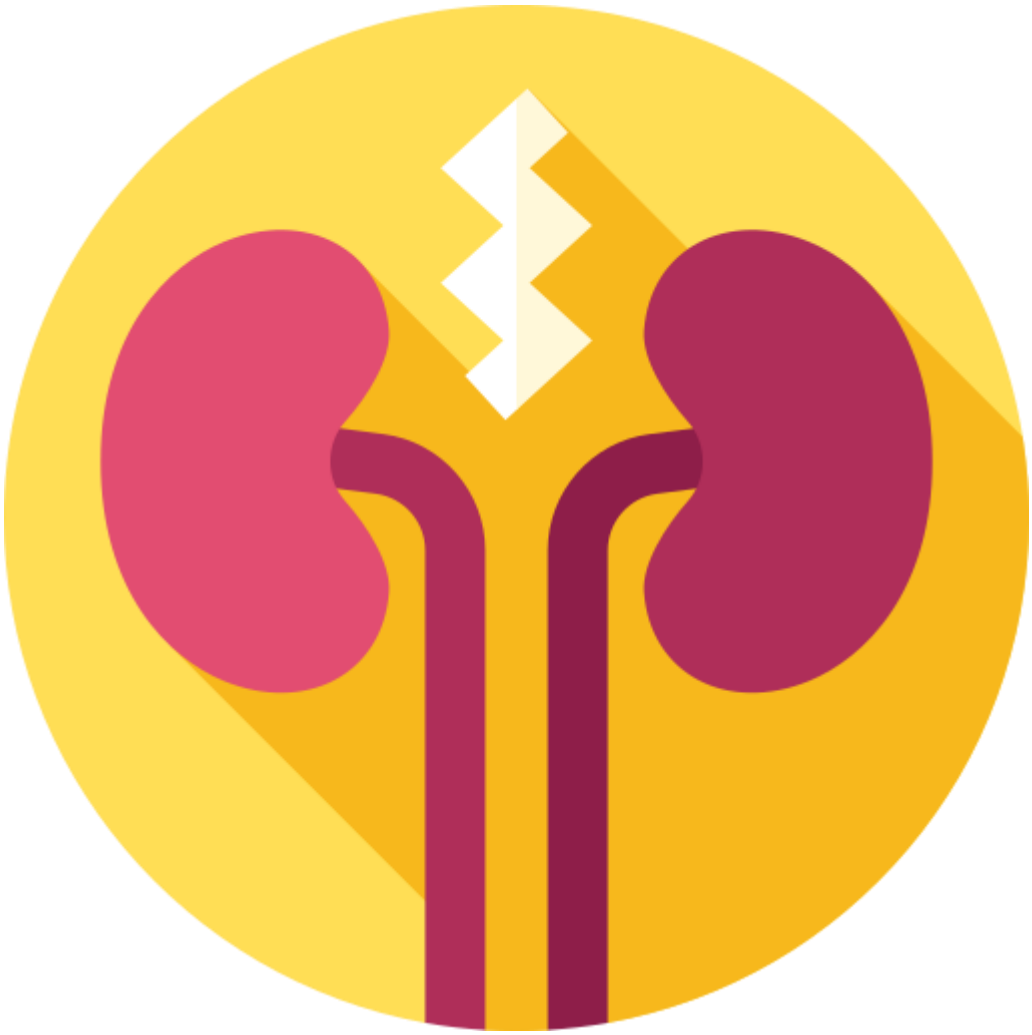

TARGETED DELIVERY OF NAVITOCLAX TO ELIMINATE SENESCENT TUBULAR EPITHELIAL CELLS

Ines Pieterman BSc

Supervisor: Yi Yang PhD
Examiners: prof. dr. R. Masereeuw & prof. dr. R. J. Kok

Abstract

Treatments for chronic kidney disorder (CKD) offer symptom management, but no cure is available. This highlights the importance of CKD prevention. The high population of senescent cells can be seen as a driver of CKD. Senescent kidney cells can be eliminated by senolytics, a class of drugs that target the anti-apoptotic pathways. Unfortunately, many senolytics are paired with severe side effects such as neutropenia and thrombocytopenia. These side effects could potentially be mitigated by linking a senolytic, navitoclax, to a small protein, lysozyme (LZM). In this study, we investigated the binding of navitoclax to LZM through the use of a platinum binder (Lx). This was done by first conjugating LZM to a methionine-ester to expose surface ligands. Next, navitoclax was linked to Lx through an S-donor bond. The last step was conjugating both pieces by linking Lx to LZM with another S-donor bond on the exposed methionine. Furthermore, we investigated whether the conditionally immortalized proximal tubule epithelial cell line overexpressing the organic anion transporter 1 (ciPTEC-OAT1), could be used as a valid in vitro model to study LZM-based delivery of a senolytic. Both binding of LZM to methionine and navitoclax to Lx were obtained of which the latter reached a 65-78% purity. Outcomes showed the complexes could not be conjugated to each other, possibly due to poor solubility, steric hindrance, or the novel binding method which uses two S-donor bonds on the Pt center. The ciPTEC-OAT1 model proved to have endocytosis-mediated uptake of LZM, and only senescent cells were susceptible to navitoclax. Therefore, the ciPTEC-OAT1 model was deemed suitable for investigating LZM-navitoclax conjugates targeted at senescent kidney cells.

Graphical Abstract

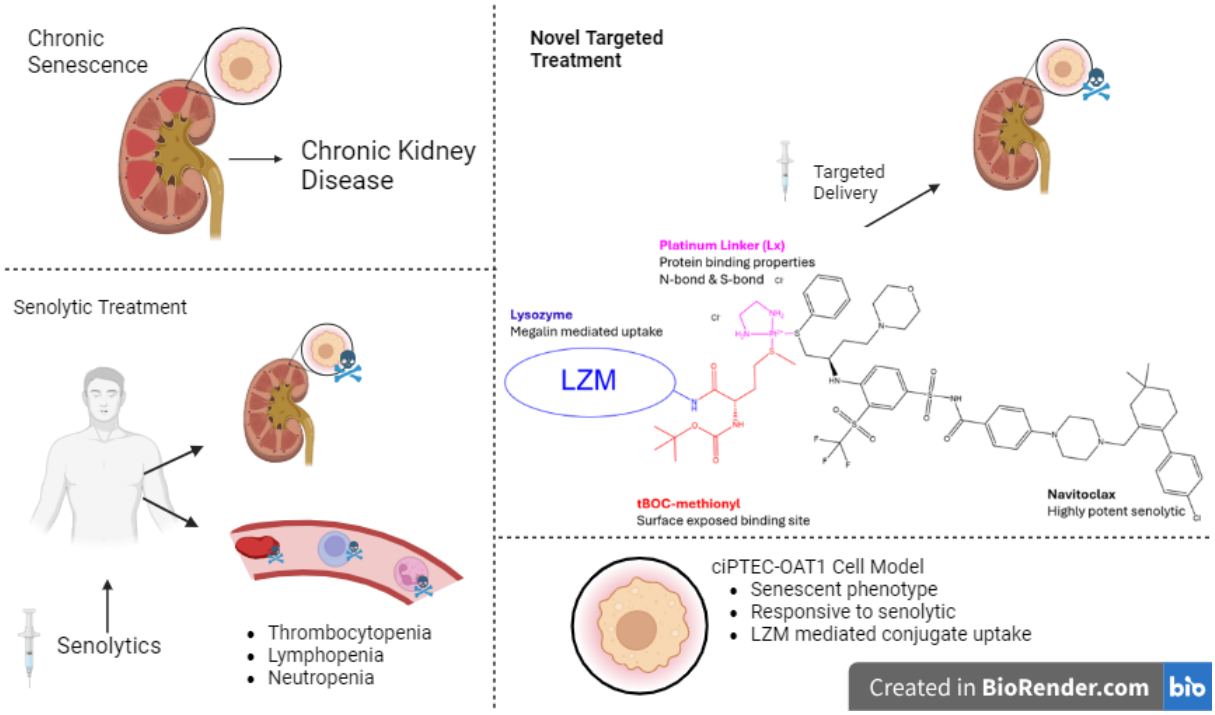

The research described in this thesis was performed in the Division of Pharmacology, Utrecht Institute for Pharmaceutical Sciences, Utrecht University.

Layman's Summary

Chronic kidney disease (CKD) is a condition in which the kidneys are failing. Current treatments are used to manage symptoms, but currently there is no cure for this disease. Because of this, it is important to prevent CKD. One major cause of CKD is a buildup of inactive damaged cells, called senescent cells. It is normal to have these cells in the body, but they grow more abundant with age. When a threshold for these cells is reached in an organ, the buildup can lead to complications such as CKD. These cells can be eliminated using a class of drugs called "senolytics". Unfortunately, these drugs can also eliminate healthy platelets and white blood cells, which may lead to serious complications.

In this study we attempt to eliminate these side effects by delivering the drug directly to the kidneys. This was done by chemically linking a senolytic called navitoclax to a small protein, lysozyme (LZM). With LZM attached to navitoclax, the drug can not enter cells and is thus inactive. LZM is small enough to be filtered by the kidneys and can enter kidney cells. Through this method, active navitoclax can kill senescent cells in the kidney while being inactive in the rest of the body, reducing side effects.

To link LZM to navitoclax we devised a method of three steps. First, modifying LZM to make it easier to bind with. Next, adding a platinum based linking molecule (Lx) to navitoclax. Lx is specifically designed to be able to link two molecules together and the third step was linking Lx on its other side to the modified LZM. Although the first two steps were successful, we were unable to complete the compound by linking navitoclax to LZM through Lx.

This study also looked at a type of senescent kidney cell (ciPTEC-OAT1) to use as a model to test how navitoclax linked to LZM would behave in the kidney. For this we tested the toxicity of navitoclax in the cells and its uptake of LZM. Results showed that these cells could absorb LZM, and that only the senescent cells were affected by navitoclax. This suggests that this cell model is suitable for further research on using LZM and navitoclax together, to target senescent kidney cells without harming healthy ones.

Generative AI

For this report generative AI was used in multiple ways. Elicit was used to help identify relevant research articles. Grammarly and ChatGPT were used to assist in writing by grammar checking, condensing and generally improving writing style. ChatGPT was also used to understand concepts and chemical reactions such as binding affinity of platinum ions and the breaking of certain bonds. All obtained knowledge was checked through published scientific articles. No generative AI was used to for data analysis, figure and/or graph generating. Furthermore, no generative AI was used for research design or idea development.

Ought. (2023). *Elicit: The AI Research Assistant* [Software]. https://elicit.com
Grammarly. (2024). *Grammarly (Version 14.1199.0)* [Software]. Grammarly Inc. https://www.grammarly.com
OpenAI. (2023-2024). *ChatGPT (Version 4.0)* [Large language model]. https://chat.openai.com

1. Introduction

Chronic kidney disorder (CKD) is a growing problem and is one of the few conditions in which death rates have gone up since 1990 (Kovesdy, 2022). With rising numbers, the incidence of CKD was at 13.4% in 2016 and is especially prevalent in aging and elderly people (Hill et al., 2016). CKD is a group of chronic disorders caused by inflammation, metabolic disorders, toxins, and other factors (Zhao et al., 2022) which results in various complications both renal and non-renal related. It can lead to early vascular aging (Dai et al., 2019), metabolic complications (Moranne et al., 2009), and progressive loss of renal functions (Chen et al., 2019). Furthermore, patients may suffer from fatigue, pain, insomnia, depression, anxiety, and general distress (Metzger et al., 2021). There is no cure for CKD and treatment options consist of symptom management such as lifestyle changes, pharmacological intervention to treat cardiovascular complications, dialysis, and in advanced cases a renal transplant (Chen et al., 2019; *Chronic Kidney Disease - Treatment*, 2017). With no cure available, prevention of CKD is of utmost importance.

Several factors can contribute to the development of CKD. One responsible factor is the accumulation of senescent cells in the kidney (Schroth et al., 2020). Senescence happens when a cell comes to a permanent growth cycle arrest. Cells becoming senescent can happen in various scenarios throughout the lifespan of tissues and organs. It can occur as a response to injury, normal organogenesis, tissue homeostasis, and repair (Docherty et al., 2019). In these cases, the senescent response is considered acute and arrested cells can be removed through apoptosis or immune clearance. Cells may also enter cell cycle arrest due to DNA damage or critical telomere shortening leading to exposure of DNA ends, oncogenic mutations, metabolic stress, mitochondrial dysfunction, and inflammation. Cells that cease proliferation through these stressors do not get cleared, as a result, they persist and accumulate within tissues and organs. This type is classified as chronic senescence and can be considered a driver of CKD when these cells accumulate in the kidneys.

Senescent cells release a unique pro-inflammatory secretome into their microenvironment called the senescence-associated secretory phenotype (SASP). This secretome can induce senescence or apoptosis in nearby cells and is considered the driver behind senescence-induced kidney fibrosis(Chaib et al., 2022; Coppé et al., 2010; Sturmlechner et al., 2017). Senescent cells are immune to the senescence-inducing proteins in the SASP through the upregulation of one or more anti-apoptotic pathways (Kirkland & Tchkonia, 2020). Although many types of renal cells can become senescent, tubular epithelial cells are most often implicated in senescence (Melk et al., 2005). Eliminating senescent tubular epithelial cells may cause senescent presence in the kidney to drop below a threshold level. Below this threshold, the body can clear senescent cells at a speed at which unhealthy accumulation is unlikely to occur and chances of senescent-induced CKD are lowered (Chaib et al., 2022).

Senescent cells can be eliminated through the use of senolytics, a class of drugs that target the anti-apoptotic pathways. Depending on the cell type several anti-apoptotic pathways can be upregulated and, in some cases, more than one pathway is overexpressed. Due to this heterogeneity in pathways a senolytic needs to be carefully selected and a combination of senolytics may be needed to eliminate senescent cells (Chaib et al., 2022; Yang et al., 2022).

In most cases senolytics only target cells that have upregulation of the targeted anti-apoptotic pathway which leads to elimination of the chronic senescent cells while non-senescent and acute

senescent cells remain intact (Fig. 1). However, senolytics that target a whole node of an anti-apoptotic pathway also cause more severe side effects (Chaib et al., 2022). Navitoclax, a first-generation senolytic, targets the anti-apoptotic Bcl-2 family. Due to its high-affinity inhibition of Bcl-2 proteins, it also induces apoptosis in platelets and lymphocytes causing thrombocytopenia and T-cell lymphopenia (Fig. 1). Furthermore, a direct side effect of inhibition of the Bcl-2 family leads to neutropenia (W. H. Wilson et al., 2010). Considering these severe side effects navitoclax is thus far inappropriate to use as a treatment option against senescent-related CKD even though in vitro studies have shown navitoclax is extremely potent in the elimination of senescent renal proximal tubule epithelial cells (Yang et al., 2022). Compared to two other senolytics, quercitin and dasatinib, that target different anti-apoptotic pathways, navitoclax has shown a greater effect in eliminating senescent cells while leaving healthy cells intact. It could prove very beneficial to investigate ways that decrease side effects while maintaining its senolytic function.

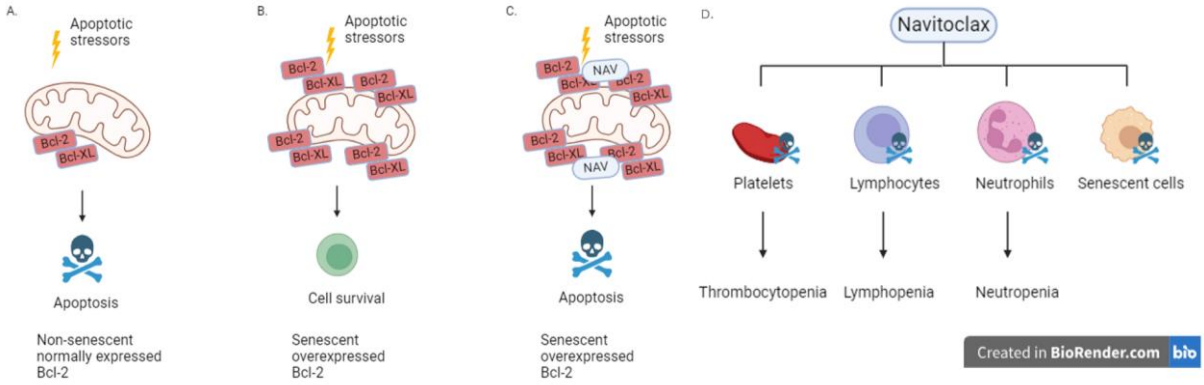

Figure 1. *Role of navitoclax in eliminating cells.* A. Normal cell entering apoptosis as a reaction on apoptotic stressors. B. A senescent cell resisting apoptosis due to the overexpressed Bcl-2 family resulting in cell survival and persistence. C. Navitoclax inhibiting Bcl-2 family proteins resulting in apoptosis of the senescent cell. D. Navitoclax induces apoptosis in cell types overexpressing the Bcl-2 family. Other than senescent cells this group also includes platelets, lymphocytes and neutrophils. The elimination of these cells leads to serious side effects.

Delivering navitoclax directly to the kidney could prevent major side effects from occurring. Navitoclax, a small molecule drug, can enter the cell freely which can cause severe effects in the body. By linking navitoclax to a small protein it would not be able to enter cells through this pathway. Lysozyme (LZM) is a small protein that naturally occurs in the body. It is taken up by proximal tubule cells through the megalin receptor after which it is degraded in the cell (Kok et al., 1998) (Fig. 2). Due to it being readily absorbed by the kidney, it has often been used in targeted delivery mechanisms to the kidney (M. E. M. Dolman et al., 2012; Haas et al., 1997; Kok et al., 1998; Wang et al., 2013; Zhang et al., 2009; Zheng et al., 2006). Navitoclax linked to LZM would not be active in the bloodstream as the conjugate is taken up by proximal tubular cells through megalin receptor-mediated endocytosis. After internalization, the drug-LZM conjugates are transported to lysosomes where they will be degraded by proteseas. Due to the degradation process, navitoclax is released from LZM and subsequently translocated to the cytosol where it can inhibit the Bcl-2 family, inducing apoptosis in the cell. Therefore, we will study the conjugation of navitoclax to LZM and the potential of LZM conjugates as an intercellular delivery method for the delivery of navitoclax in in vitro cultured senescent kidney cells.

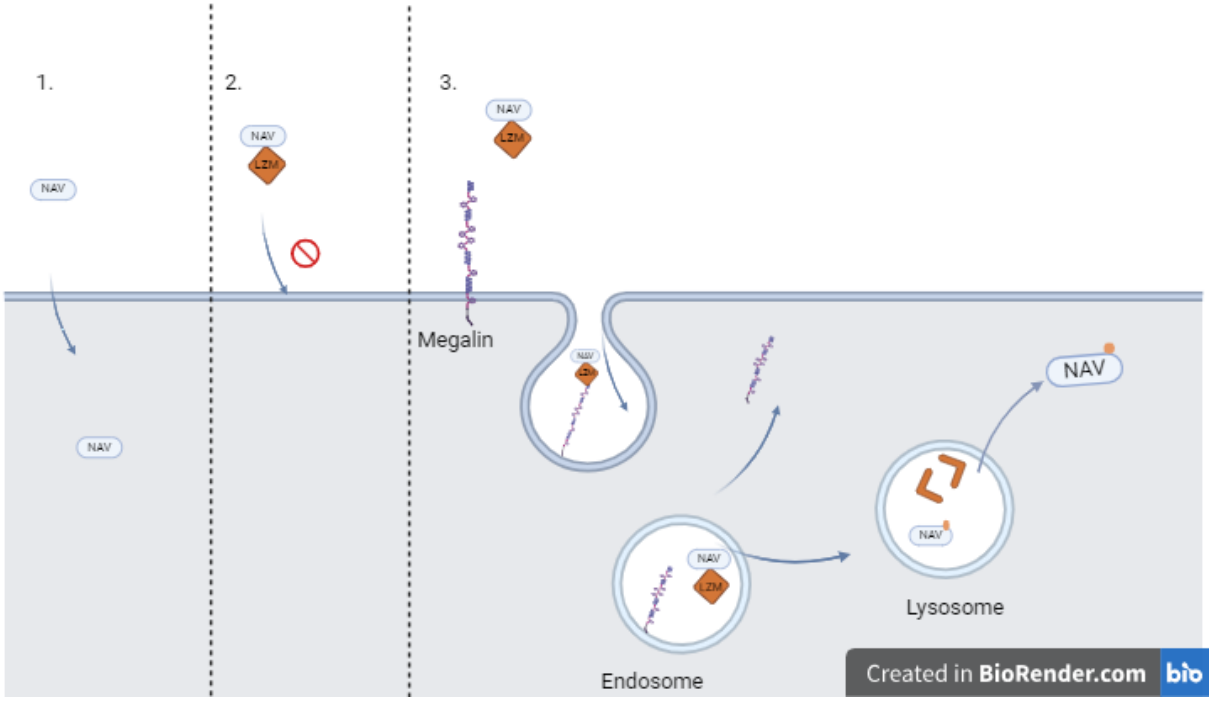

Figure 2. *Cell entry of navitoclax.* 1. Navitoclax is passively taken up by both nonsenescent and senescent cells. 2. Navitoclax conjugated to LZM can not pass the cell membrane. 3. When megalin is present on the cell membrane the navitoclax-LZM conjugate can enter the cell through receptor mediated endocytosis. In the lysosome the low pH degrades LZM and active navitoclax can enter the cytosol.

The linking of navitoclax to lysozyme can be done through a platinum-based linker (Lx). This linker has been used in renal in-vivo studies using drug-protein conjugates and drug-folate conjugates (M. E. M. Dolman et al., 2012; Shi et al., 2018). The use of Lx as a linker to LZM has already been established and conjugates have proven stable and non-toxic in mice (Prakash et al., 2006; Waalboer et al., 2015; J. J. Wilson & Lippard, 2014). Furthermore, the introduction of the charged linker increases the solubility of navitoclax (Waalboer et al., 2015). Lx has two linker sites that can be linked to S-donor or the more stable N-donor ligands (Merkul et al., 2019; Waalboer et al., 2015). Lx can link to naturally occurring amino acids such as methionine (Waalboer et al., 2015) but with LZM these ligands are hidden within the protein making them unsuitable. Therefore, methionine residues are introduced at the surface of the protein (Prakash et al., 2006). Most drug-Lx-protein complexes are made using one N-bond and one S-bond but considering the best available ligand on navitoclax is an S-donor, we will use the novel approach of a dual S-bond. The conjugation will be a three-step process: 1. Lysozyme-methionine (LZM-m), 2. Navitoclax-Linker (Nav-Lx), and 3. LZM-m-Lx-Nav (Fig. 3).

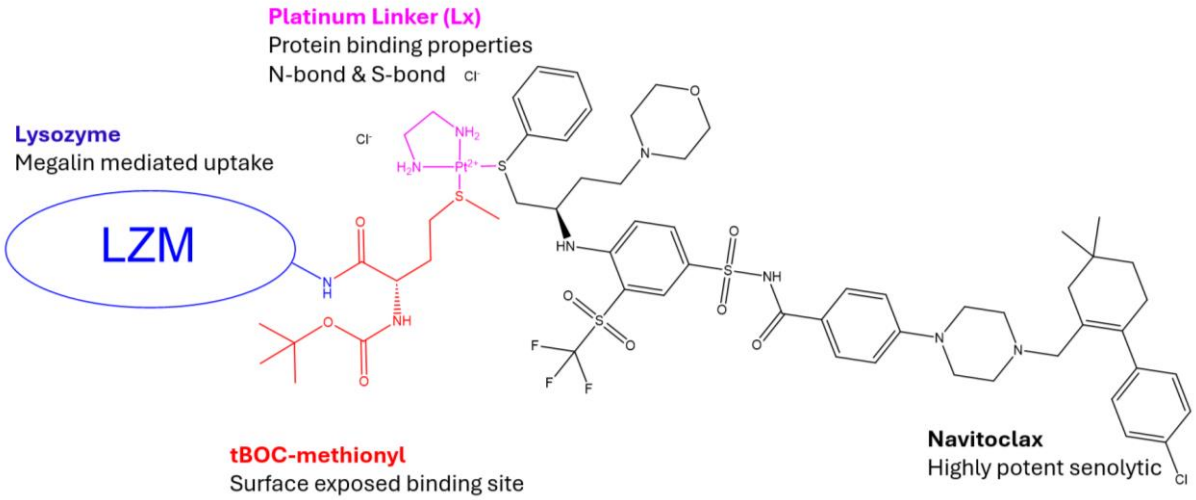

Figure 3. *Proposed final conjugate consistent of four parts.*

Our research group has previously shown that conditionally immortalized proximal tubule epithelial cell line equipped with organic anion transporter 1 (ciPTEC-OAT1) can be used as a study model to investigate senescence and senolytic response (Yang et al., 2022). Temperature-sensitive SV40T allows cells to proliferate at the permissive low temperature of 33°C but induces a proliferation block that resembles senescence at a non-permissive temperature of 37°C (Wilmer et al., 2010; Yang et al., 2022). Maturing the cells for 9 days at 37°C promotes senescent features e.g., upregulation of SASP, SA-β-gal expression, and apoptosis-associated proteins Bcl-2, BID, and Bax (Yang et al., 2022). Furthermore, ciPTEC-OAT1 has shown to be susceptible to senolytic response including navitoclax making this cell model a highly suitable candidate for testing the LZM-m-Lx-Nav conjugate. CiPTEC-OAT1 has not been used before as a model for testing LZM-mediated drug uptake, additional tests are in place.

In this study, we explore the option of eliminating senescent proximal tubular epithelial cells in the kidney through an LZM-based delivery method. To achieve the delivery system, we will attempt to link Navitoclax through a platinum linker to LZM. We will investigate the binding ability of navitoclax to Lx, the binding of LZM to a methionine ester, and finally the binding between Nav-Lx and LZM-m. To map the suitability of the ciPTEC-OAT1 as a cell model to study LZM-mediated delivery of a senolytic to eliminate senescent tubular epithelial cells, we will study the uptake of LZM in ciPTEC-OAT1 through fluorescently labeled LZM.

2. Methods

2.1 Synthesis

UPLC Analysis

To determine the success of reactions, UPLC was performed on an Acquity waters UPLC BRH c18 1.7um (2.1 x 50mm) column and detected using UV/vis or fluorescence. The method was set at 100% eluent A (H_2O/ACN (95/5 %) + 0.1% formic acid (FA)) at timepoint 0.00min to 100% eluent B (ACN + 0.1% FA) at timepoint 8.00min, at a flow rate of 0.5 mL/minute. Freeze dried samples were dissolved and diluted to a concentration of 0.33 mg/mL using eluant A. Water insoluble compounds (navitoclax, nav-Lx, RBITC) were first dissolved in DMF before diluting with eluant A. Injection volume was set at 5µL. To characterize compounds, retention times of peaks were compared to unreacted starting compounds. This UPLC protocol was used for all compounds with changes to detection settings, UV/vis was read at 318nm for navitoclax, 280 for LZM, and fluorescence at λ_{ex} 543 nm, λ_{em} 580 nm for rhodamine-b-isothiocyanate (RBITC). All chromatograms were analysed using Empower Software.

Mass Spectometry

UPLC coupled to a QTOF mass spectrometer (MS) equipped with electrospray ionization (ESI) was used to collect MS data. An ACQUITY UPLC CSH C18 column (2.1 × 50 mm) was used for separation. Solvents are identical to UPLC method, binary solvent of H_2O/ACN (95/5 %) + 0.1% FA and 100% CAN + 0.1% FA as the mobile phase. Mass analysis was conducted in positive ionization mode. Data was analyzed using Agilent MassHunter workststation Qualitative Analysis version 10.0. Theoretical m/z were compared to obtained m/z, data was only used for qualitative analysis.

RBITC-LZM

RBITC was linked to LZM to function as a label to determine the uptake of LZM in senescent ciPTEC (Fig. 4).

A 10 mg/mL solution of RBITC in DMF was slowly added to a 5mg/mL solution of LZM in PBS in a molar ratio of 3:1 (RBITC:LZM). It was reacted for 1 hour at room temperature under gentle magnetic stirring. To remove excess RBITC, the solution was filtered through a 0.45 um RC filter and then dialyzed using Spectrum™ Spectra/Por™ 3 RC Dialysis Membrane Tubing with a 3500 Dalton MWCO and a diameter of 11.5 mm. Dialysis was done 4 times against 5L ultrapure water and resulting dialyzed product was subsequently lyophilized and stored at -20 ℃. RBITC-LZM was characterized using UPLC by comparing retention times of peaks to starting compounds. QTOF-MS was performed on sample to determine reaction products.

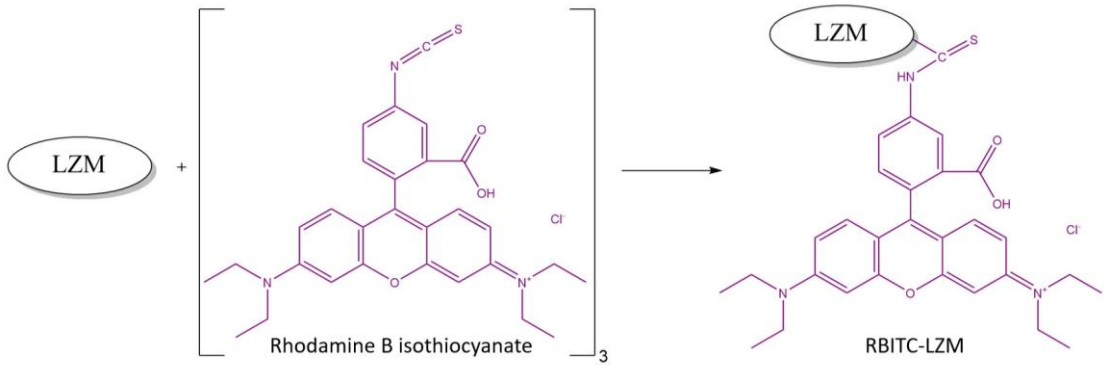

Figure 4. *Reaction scheme for the synthesis of RBITC-LZM.*

Stability Test

The stability of RBITC-LZM conjugate was tested by dissolving the conjugate in HBSS buffer and incubating it at 37°Cor 4°C for 0, 2, 6, 24, 30, or 53 hours. Samples were analyzed using UPLC to monitor fluorescence activity corresponding to the release of rhodamine derivatives, outside of the retention time window of intact RBITC-LZM (timepoint 0h).

LZM-Methionine

To prepare LZM for binding to navitoclax it is first reacted to Boc-L-methionine N-hydroxysuccinimide (methionine) according to literature (M. E. M. Dolman et al., 2012)(Fig. 5). A 10 mg/mL solution LZM in PBS was reacted to a three times molar excess 15 mg/mL solution Boc-L-methionine N-hydroxysuccinimide in DMF at room temperature for one hour under gentle magnetic stirring. The solution was purified through dialysis, four times against 5L ultrapure water, and subsequently lyophilized and stored at -20℃. LZM- Boc-L-methionine N-hydroxysuccinimide (LZM-m) was characterized using UPLC-UV and QTOF-MS.

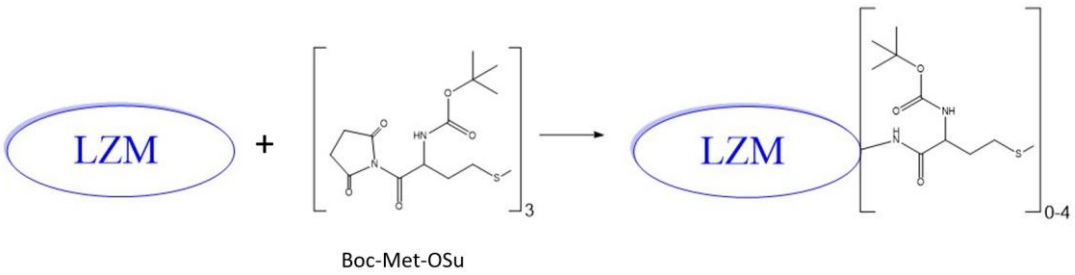

Figure 5. *Reaction scheme for the modification of LZM with methionine.*

Navitoclax-Lx

Platinum Linker

[PtCl(ethylenediamine)NO3] (Lx) was synthesized by reacting [PtCl2(en)] (250 mg, 0.769 mmol) with AgNO3 (130 mg, 1 equiv) in 10 ml DMF overnight in the dark at room temperature. The formed AgCl precipitate was removed by filtration through a PTFE filter (0.2 µm, 47 mm diameter, Whatman).

Linking of Lx and Navitoclax

To link navitoclax to Lx to form nav-Lx (Fig. 6), navitoclax in DMF (10mM, 5µM) was reacted to Lx in a 2.5 times molar excess at both room temperature and for a duration of 72h. Method development is described in supplementary information. UPLC was performed to determine the outcome and preparative HPLC was performed to separate compound peaks. Products were separated using a GRACE Alltima C18 column (250 mm length, 22 mm internal diameter, 5 µm particle size) equipped with a matching precolumn. The mobile phase consisted of Eluent A (100% H_2O with 0.1% formic acid) and Eluent B (100% acetonitrile with 0.1% formic acid). A gradient elution was used, starting with 80% A and 20% B, gradually shifting to 40% A and 60% B over 60 minutes. The column was subsequently re-equilibrated to initial conditions over the next 2 minutes and flushed with 100% A at the end of the run. The total run time was 60 minutes. Flow rate was set at 10 mL/min, and detection was performed using a UV detector at 318 nm. The injection volume was 4 mL of sample, prepared by diluting 400 µL of the reaction mixture (lyophilized reaction product dissolved in DMF in a concentration of 0.66 mg/mL) with 3600 µL of Eluent A.

After separation on the preparative HPLC column, the product was collected manually by monitoring the chromatogram. Peaks corresponding to the target compound, Nav-Lx, were identified based on retention time and UV absorbance at 318 nm and were eluted from the column between 20-30 min. All fractions were collected and pooled for further analysis using UPLC to determine target compound Nav-Lx.

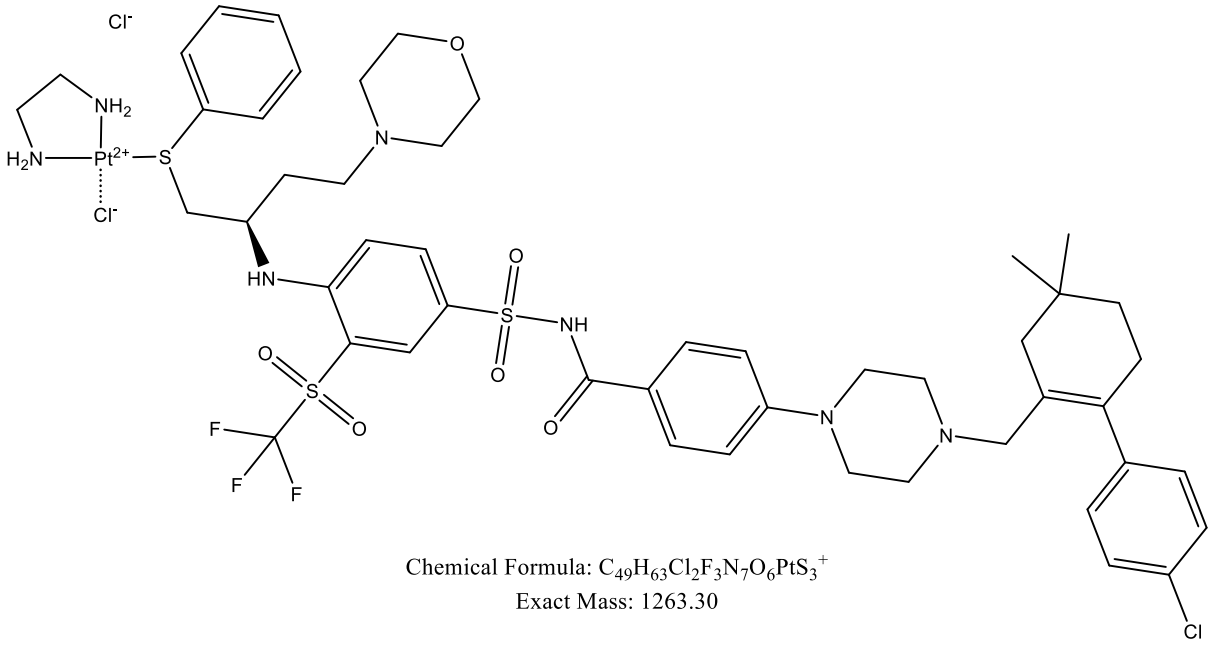

Figure 6. *Nav-Lx with its chemical formula and molecular weight.*

Dissociation Assay

To confirm successful linking between navitoclax and Lx a potassium thiocyanate (KSCN) dissociation assay was performed. 10 mg/mL conjugate was dissolved in DMF and treated with 9.6 mM of KSCN in DMF and reacted at 80°C for 2h to release navitoclax from the linker. Free navitoclax was measured using UPLC.

LZM-m-Lx-Navitoclax

To form the final conjugate (Fig. 7), LZM-m was dissolved in HEPES (20mM HEPES buffer pH 8.5) and reacted to Nav-Lx overnight at 37°C in a 1:2 molar ratio. The sample was subsequently dialyzed (MWCO: 3.5K) against HEPES (20 mM HEPES buffer pH 7.5), overnight. The buffer was replaced two times. The product was stored at -20°C and analyzed using ULPC.

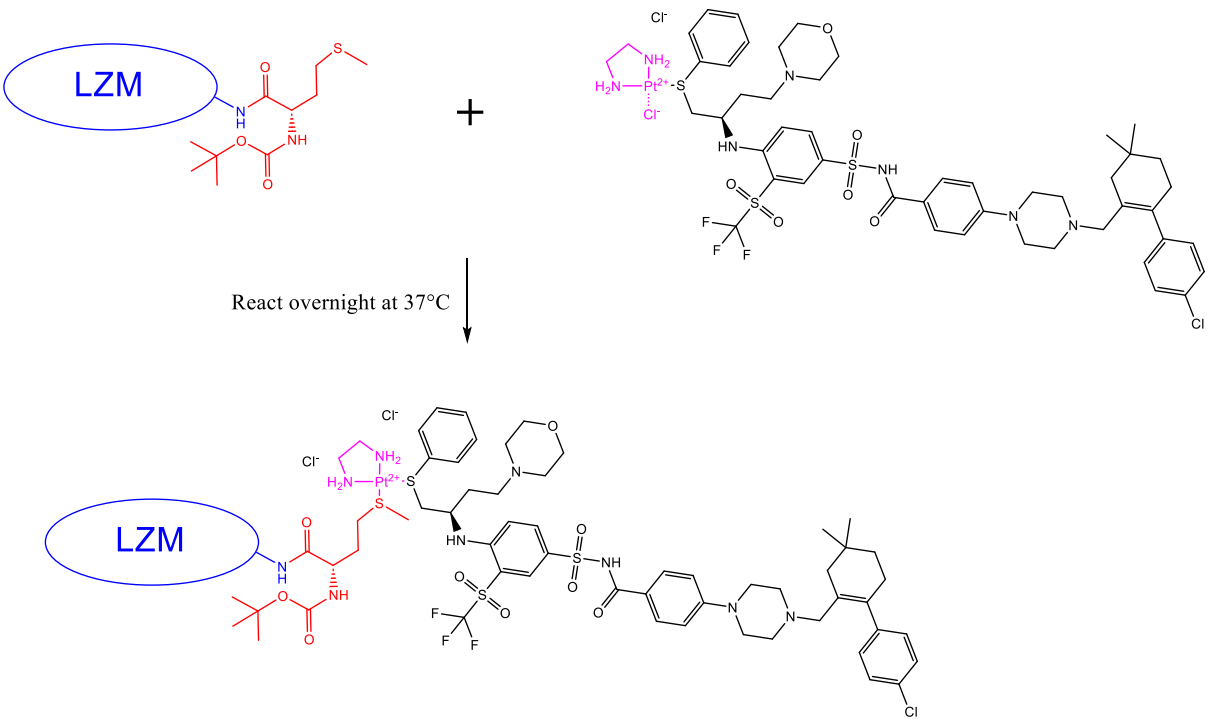

Figure 7. *Reaction scheme for the synthesis of LZM-m-Lx-Nav.*

LZM-m-Lx

For this experiment, LZM-m was dissolved in HEPES (20 mM HEPES buffer pH 8.5). Dissolved LZM-m was reacted to Lx overnight at 37°C in a 1:1 and 1:5 molar ratio. Samples were stored at -20°C and analyzed using ULPC.

LZM-m-Lx-Lissamine

To track how a platinum-linked drug-lysozyme conjugate behaves in senescent ciPTEC, LZM was linked to a fluorescent tag using Lx, a complex shown in Figure 8. Lissamine, a fluorescent dye, was linked to Lx via a hydrophilic spacer (Shi et al., 2018). Lissamine-Lx was provided by LinXis in lyophilized form.

LZM-m was dissolved in HEPES (20mM HEPES buffer pH 8.5) and reacted to Lissamine-Lx dissolved in DMF, overnight at 37°C in a 1:1 molar ratio. Samples were stored at -20°C and analyzed using ULPC.

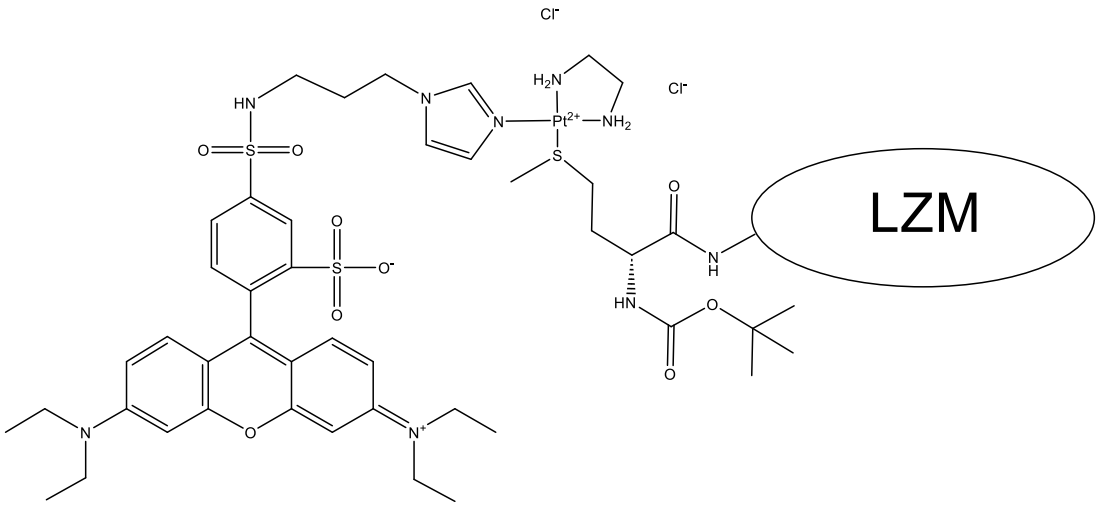

Figure 8. *Lissamine-Lx-m-LZM.*

2.2 In Vitro

Culturing and maturing of ciPTEC

Handling of ciPTEC-OAT1 was done as described elsewhere (Yang et al., 2022). All in-vitro experiments used ciPTEC-OAT1 cells which were cultured in DMEM/F12 supplemented with 10% (v/v) fetal calf serum, 5 µg/ ml insulin, 5 µg/ml transferrin, 5 µg/ml selenium and 10 ng/ml epidermal growth factor (EGF). The medium was refreshed every 2-3 days and the passage of cells was between 40 and 60. Cells were cultured at 5% (v/ v) CO2 at 33°C and at 37°C to allow for proliferation and maturation respectively. All experiments were performed in three and three independent experiments were performed.

Senescence cell viability assay

To confirm the toxicity of navitoclax in senescent ciPTEC-OAT1a viability assay using presto blue was performed on senescent and non-senescent like ciPTEC. Cells were seeded in a 96-well plate at a density of 63,000 cells per square cm after which plates were set at 33°C for 24h to proliferate. To induce senescence, plates were further incubated at 37°C for an additional 8 days to allow for maturation. Cells were exposed to medium with navitoclax in the range of 1-3000 nM for 24h at 37°C for senescent ciPTEC-OAT1 and 33°C for non-senescent ciPTEC. A PrestoBlue cell viability kit was used per kit instructions.

LZM uptake in senescent ciPTEC

Uptake of LZM in senescent ciPTEC-OAT1 was monitored using LZM tagged with the fluorescent label RBITC (LZM-RBITC). The Fluorescence of RBITC is pH insensitive making it a suitable label to determine endocytosis-mediated uptake as the acidic environment in the lysosomes will not affect fluorescence (Rizzo et al., 2022).

Incubation time

The effect of time on LZM uptake was measured using an uptake assay. Cells were seeded in a 96-wells plate at a density of 63,000 cells per square cm after which plates were set at 33°C for 24h to proliferate. To induce senescence, plates were further incubated at 37°C for an additional 8 days. Medium with RBITC or RBITC-LZM was introduced to the cells at 35.0, 25.0, 17.5, 12.5, 8.75, 6.25, 4.38, 3.13 and 0 mg/ml for RBITC-LZM and 11.2, 8.0, 5.6, 4.0, 2.8, 2.0, 1.4, 1.0 and 0 mg/mL for RBITC. Plates were subsequently incubated at 37°C for a duration of 1h, 3h, or 6h. After incubation cells were thoroughly washed using cold HBBS to remove any excess. Cells were lysed using TRITON-1% and plates were read at excitation, 543 nm; emission, 580 nm.

Temperature

As megalin-mediated uptake is temperature dependent, the effect of temperature on the uptake of LZM in ciPTEC-OAT1 was determined to confirm uptake of LZM is done through the megalin receptor. Cells were seeded and treated as described in the time assay with some alterations. Incubation with RBITC/RBITC-LZM was set at 3h and took place at 37°C and on ice.

Inhibition assay

To further determine megalin mediated uptake a competitive inhibition using LZM was performed. Plates were prepared as mentioned above and cells were treated with RBITC-LZM (12.5 mg/mL) or Rhodamine B (RB, 2mg/mL). Both groups of cells were treated with free LZM in a molar excess (RBITC-LZM/RB: LZM) range of 1:2, 1:3, 1:4, 1:5, 1:6, 1:8, and 1:10 (1.62, 2.44, 3.25, 4.06, 4.87, 6.50 and 8.12 mM of LZM). Plates were incubated for 3 hours at 37°C.

Statistical Analysis

All data analysis and statistics were performed using the GraphPad Prism (version 9.3.1; GraphPad Software, La Jolla, CA), and expressed as mean ± SEM. A comparison of two groups at different temperatures and different time points was done using two-way ANOVA, followed by Sidak's multiple comparison test. $P < 0.05$ was considered significant. Cell viability was expressed as inhibitory constants at 50% of control viability levels (IC50 values), which were calculated by plotting log navitoclax concentration vs. viability following background subtraction. Uptake was expressed as an increased percentage of fluorescence as compared to the lowest concentration

3. Results

3.1 Synthesis

RBITC-LZM

Stability Test

As seen in Figure 9, incubation at 37°C resulted in a decrease in the first shoulder of the peak and an increase in the latter. A reconfiguration of the RBITC molecules to LZM would have resulted in free rhodamine derivatives. No free rhodamine was observed making it likely this change was due to a conformational change of RBITC-LZM. Furthermore, the chromatogram only showed two peaks while LZM has up to 7 attachment sites for RBITC. Therefore, making us conclude the observed peaks are due to a change in protein folding and not its degree of modification as that would result in more peaks. This conformational change was not observed when incubated at 4°C. At both temperatures and all incubation times, the conjugate was stable and no free RBITC was detected.

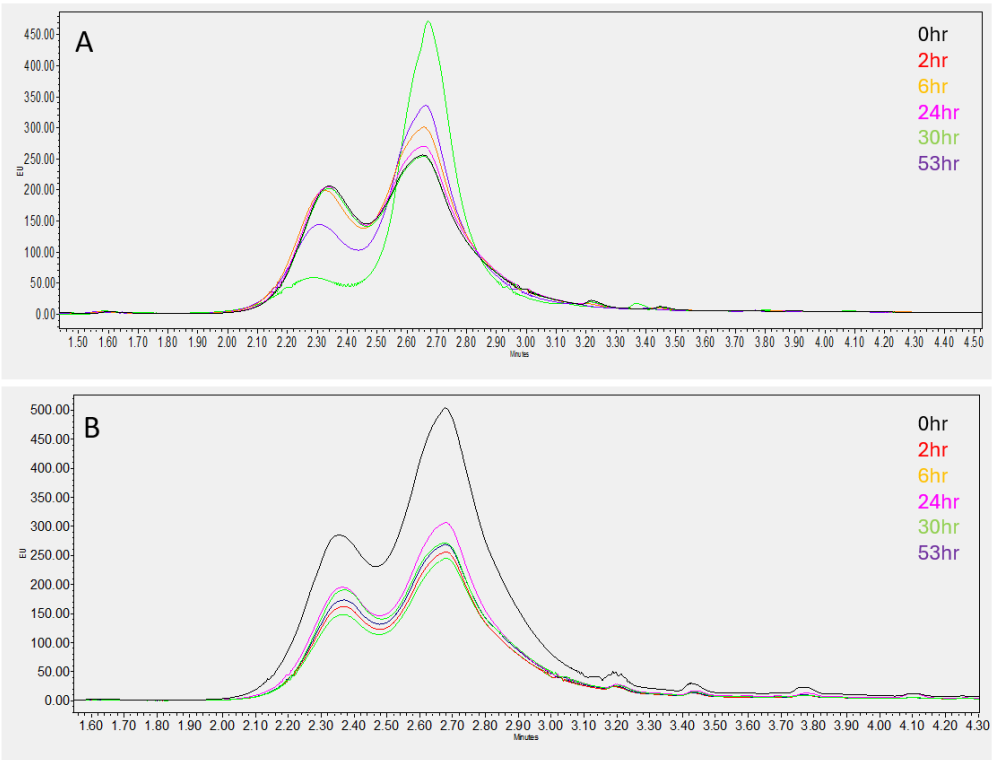

Figure 9. *UPLC characterization of RBITC-LZM after time exposure of 0, 2, 6, 24, 30 and 53 hours*. A. At 37°C, no free RBITC is observed at any time point. Longer exposure times, 30h (green) and 53h (purple) showed a slight decrease in the first shoulder of the RBITC-LZM peak and an increase in the second shoulder, most likely due to a conformational change. Other times, 0h (black), 2h (red), 6h (orange), and 24h (pink), did not show this difference. B. at 4°C, no free RBITC or confirmational change was observed at any time point.

LZM-Methionine

UPLC showed a slightly longer retention time and the lysozyme conjugate showed 5 peaks (Fig. 10). This is consistent with existing data, in which 0, 1, 2, 3 or 4 methionine residues bind to one molecule of lysozyme using this protocol (M. E. M. Dolman et al., 2012). This was further confirmed by MS (Fig. S4)

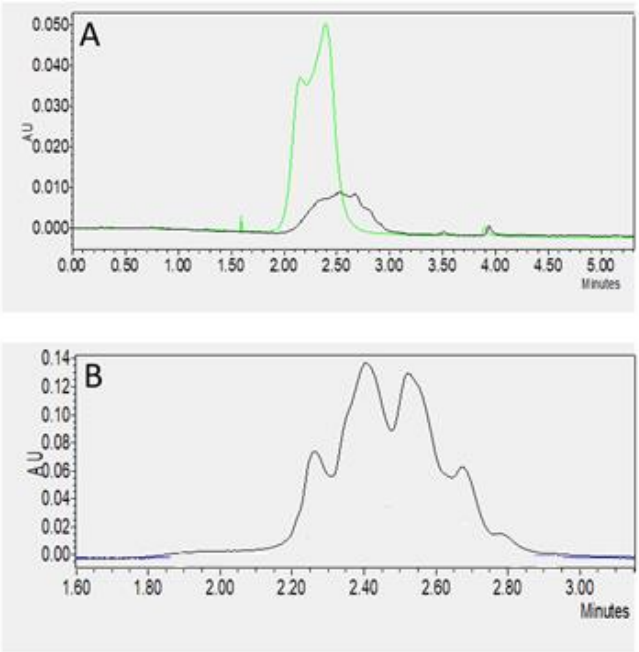

Figure 10. *UPLC chromatogram of LZM and modified LZM*. A. Methionine modified LZM (black) and unmodified LZM (green). B. LZM-m peak is comprised of 4 peaks.

Navitoclax-Lx

Linking of Lx and Navitoclax

UPLC showed linking of Lx to navitoclax resulted in several peaks as shown in Figure 11. Two of those peaks, 3 and 4, were possible compounds of interest. Dissociation assay (Fig. 12) and QTOF-MS (Fig. S5) showed peak 3 was nav-Lx and peak 4 was an unreactive fragment of navitoclax.

After preparative HPLC a compound with an average purity of 71.5% (n=2) was obtained according to the AUC% based on peak integration of the UPLC chromatograms (Fig. S6).

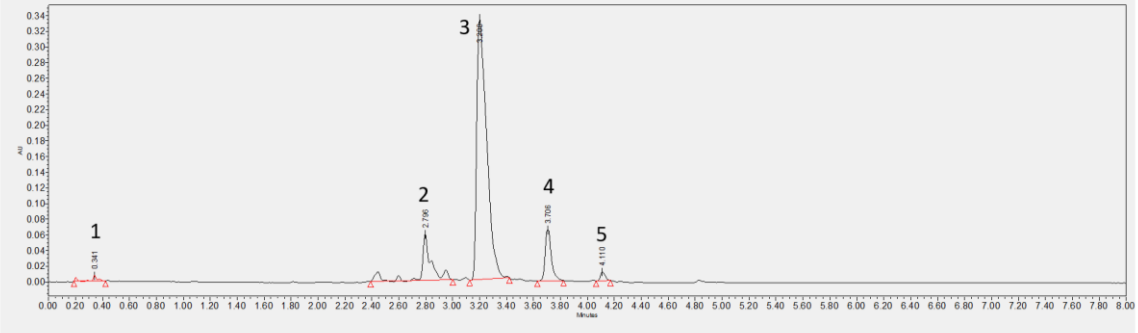

Figure 11. *UPLC characterization of nav-lx. The reaction was performed at room temperature for 3 days and separated using HPLC prep*. Peak 1: free Lx, peaks 2 & 4: navitoclax fragments, peak 3: nav-Lx, and peak 5: navitoclax.

Dissociation Assay

Using the competing platinum ligand, KSCN, in a dissociation assay showed no effect on peak 4, indicating no bond was formed between Navitoclax and Lx (Fig. 12B). When performed on peak 3, the dissociation assay showed all compounds from peak 3 had turned into free navitoclax (Fig. 12A).

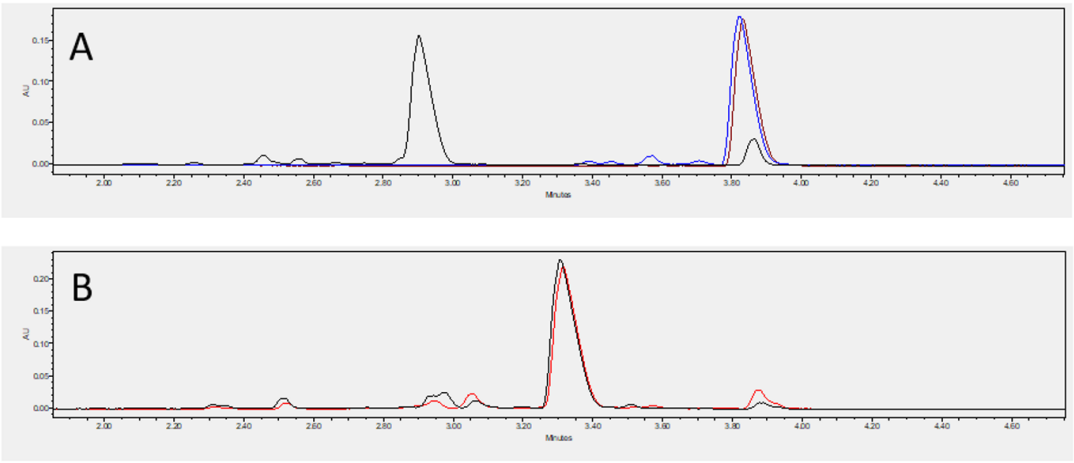

C $\quad Nav\text{-}Lx\text{-}Cl + 2KSCN \rightarrow Lx(SCN)_2 + Nav + 2K^+ + Cl^-$

Figure 12. *UPLC characterization of the KSCN dissociation assay. A*. untreated nav-Lx (black) as compared to nav-Lx treated with KSCN (blue). Navitocax (purple) as a reference compound. B. Fragmented Navitoclax (black) as compared to fragmented navitoclax with KSCN (red). C. The reaction scheme of the KSCN dissociation assay as performed on Nav-Lx.

LZM-M-Lx-Navitoclax

UPLC showed no new peaks were formed when LZM-m was reacted to Nav-Lx (Fig. 13). Nav-Lx (peak 1) did decrease slightly during the reaction while free navitoclax (peak 2) increased.

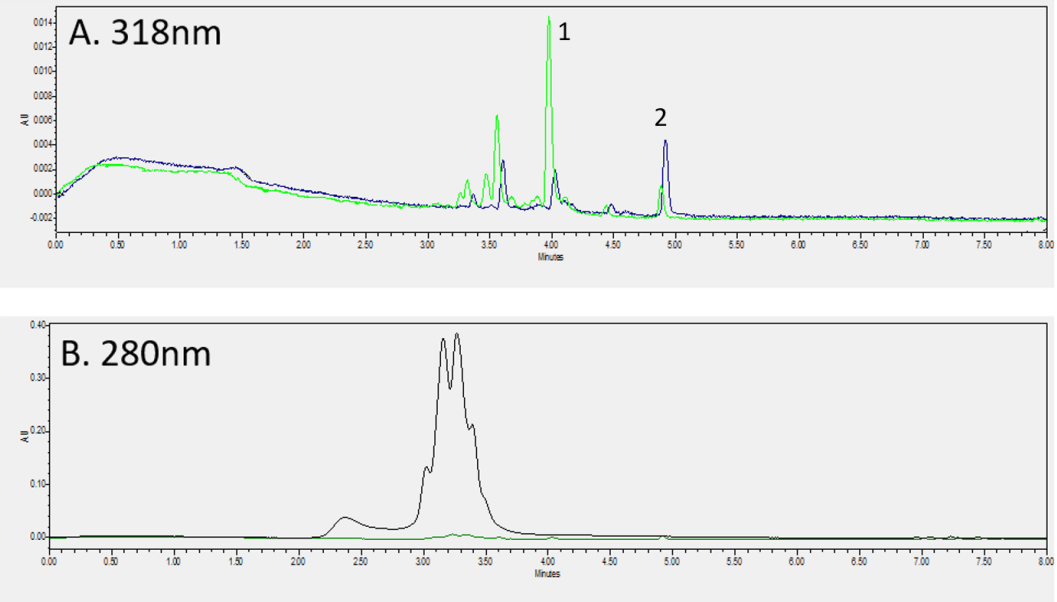

Figure 13. *UPLC reaction of LZM-m reacted with nav-Lx.* A. unreacted nav-Lx (green) and nav-Lx reacted with LZM-m. Peak1: Nav-Lx, Peak 2: navitoclax. B. LZM-m.

LZM-m-Lx

When reacting LZM-m to Lx in a 1:1 ratio, little reaction was seen. UPLC showed no change in retention time (Fig. 14). However, at 5 times molar excess of Lx, UPLC showed a shorter retention time indicating successful conjugation. The presence of HEPES during the reaction did not affect conjugation.

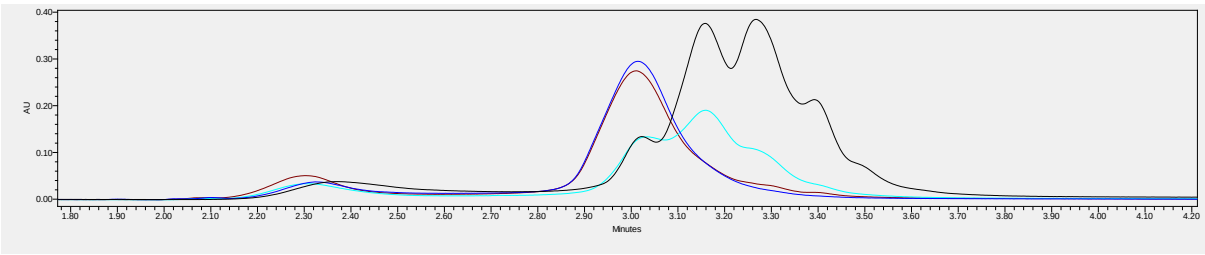

Figure 14. *UPLC characterization of Lx reacted to LZM-m.* LZM-m (black), LZM-m: Lx 1:1 (cyan), LZM-m: Lx 1:5 (blue), LZM-m: Lx 1:5 no HEPES (brown).

LZM-m-Lx-Lissamine

MS showed successful conjugation of LZM-m to Lissamine-Lx (Fig. S7). Results were not quantified but MS showed LZM-m not bound to Lissamine and LZM-m bound to one, two or three molecules of Lissamine. Successful conjugation suggests there are no issues with the binding properties of LZM-m and the problem with conjugation between Nav-Lx and LZM-m lies with Nav-Lx. There are two major differences between Nav-Lx and Lissamine-Lx. Lissamine is bound to Lx through an N-bond while navitoclax is bound through an S-bond to Lx. Secondly, navitoclax is directly linked to Lx but there is a small spacer between lissamine and Lx (Fig. 8).

3.2 In Vitro

Effect of Navitoclax on ciPTEC

Senescence-like ciPTEC-OAT 1 are susceptible to navitoclax

Toxicity of navitoclax in senescent ciPTEC-OAT1 was established. Cell viability assay (Fig. 15) showed that navitoclax had a cytotoxic effect on senescent ciPTEC-OAT1 with an LC50 of approximately 1 mM. No toxicity was measured if the ciPTEC-OAT1 were in their permissive non-senescent state. This shows that navitoclax is a useful agent in selectively eradicating senescent cells.

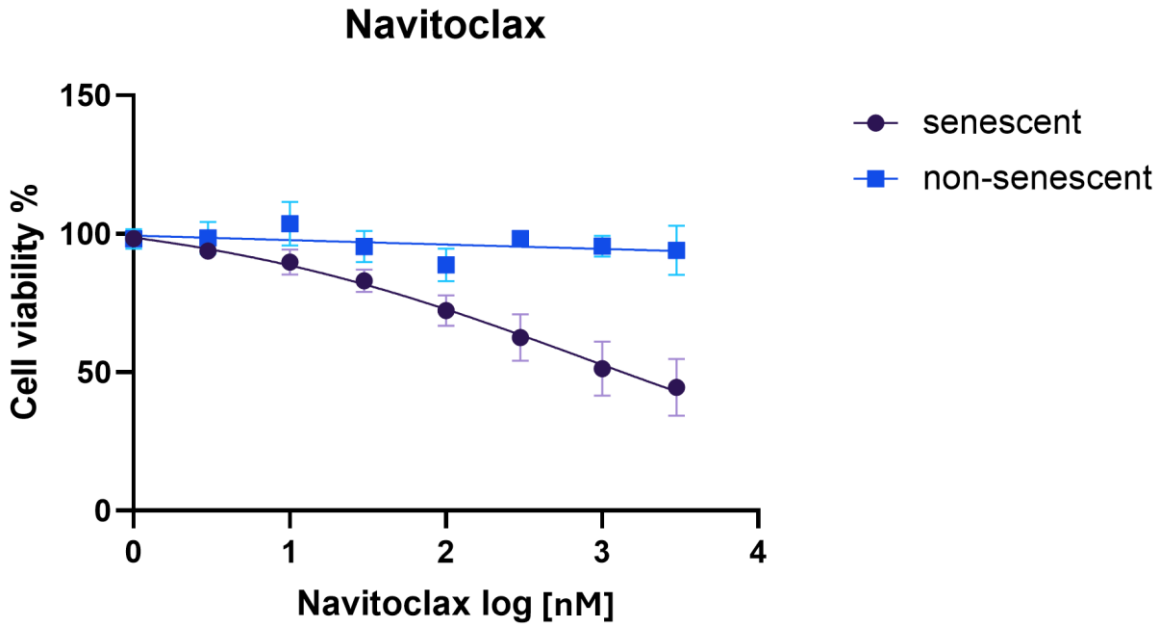

Figure 15. *Effect of navitoclax on cell viability of ciPTEC-OAT1 in the senescent and non-senescent state.*

Uptake of LZM by senescence-like ciPTEC-OAT 1

Some studies have shown that megalin expression is low in ciPTEC-OAT1 although it does show time-dose dependant uptake of albumin and receptor-associated-protein (RAP) (Caetano-Pinto et al., 2016; Sun et al., 2020; Wilmer et al., 2010) which does not take place in megalin-deficient cells (Caetano-Pinto et al., 2016). For this reason, we will study the uptake of LZM in ciPTEC-OAT1 using fluorescently labelled LZM to determine if uptake is done through receptor-mediated endocytosis. Figure 16 shows how megalin mediated uptake should occur.

The incubation time assay showed uptake of the fluorescently marked LZM was good and presented in a dose-dependent manner (Fig. 17A). Uptake of RBITC-LZM was considerably higher when incubated for 3 hours as compared to a 1-hour incubation time. However, increasing the time to 6 hours seems to have little effect on uptake. In figure 17B, it shows that ciPTECs also take in free RBITC. At an incubation time of 1h, this is done in a dose-dependent manner but at longer incubation times this trend fades. RBITC can freely react to surrounding proteins, this change can partly be explained by RBITC reacting to the cell membrane or other medium components upon introduction, which is no longer reactive after an hour. However, due to the decline in intracellular RBITC levels we suspect that the low molecular weight RBITC is exiting the cells. Uptake of RBITC-LZM is much greater as compared to RBITC uptake indicating different uptake mechanisms are in play. Further studies to characterize RBITC-LZM uptake were done using an incubation time of 3 hours

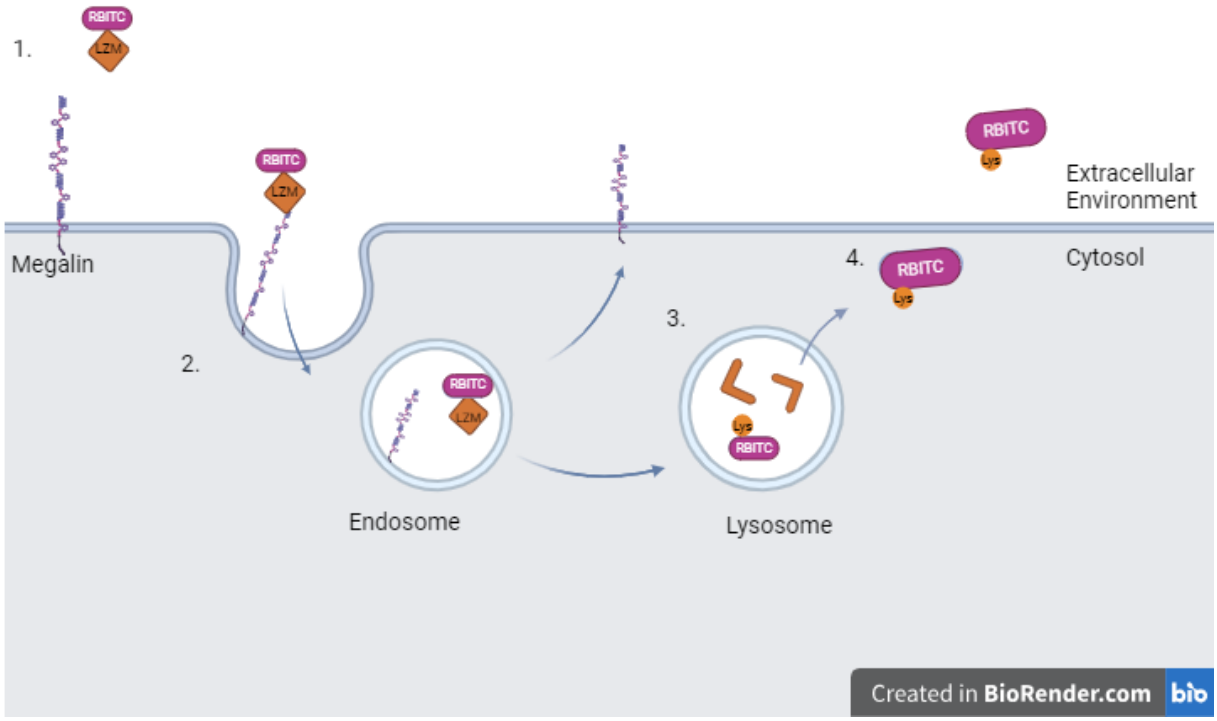

Figure 16. *Megalin-mediated uptake of RBITC-LZM.* 1.) Megalin present on the outside of the cell membrane detects RBITC-LZM. 2). Megalin and RBITC-LZM complex internalize from the membrane and move to the endosome. The drop in pH disrupts binding of the receptor with RBITC-LZM and megalin is recycled back to the membrane. 3). Endosome fuses with a lysosome, low pH and lysosomal enzymes degrade RBITC-LZM. Peptide bonds are broken, leaving RBITC-Lysine (RBITC-Lys). 4). RBITC-Lys leaves the lysosome by diffusing over the membrane and enters the cytosol.

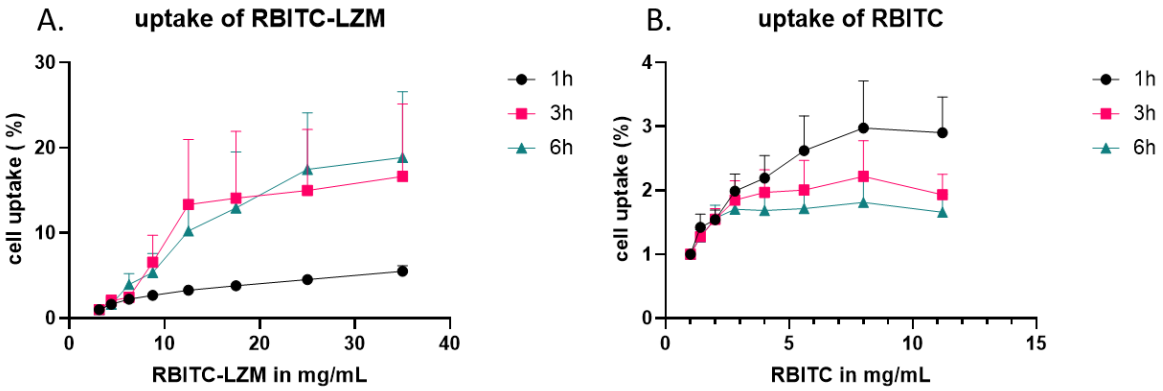

Figure 17. *Uptake of RBITC-LZM (A) and RBITC (B) in senescent ciPTEC-OAT1 after incubation of 1, 3, or 6 hours.* Medium with RBITC or RBITC-LZM was introduced to the cells in a range of 0-11.2 mg/mL and 0-35 mg/mL respectively.

Uptake of LZM in senescent ciPTEC-OAT1 is receptor-mediated.

To further investigate whether the uptake of RBITC-LZM is done through endocytosis, the uptake was studied under different temperatures. Uptake of RBITC-LZM presented in a dose-dependent fashion for both temperature points but a statistical difference in uptake was observed (Fig. 18). At 4°C there was very little uptake of the LZM-conjugate, indicating that due to the low-temperature uptake was impacted. RBITC uptake did not decrease due to low temperature, in the contrary uptake went up.

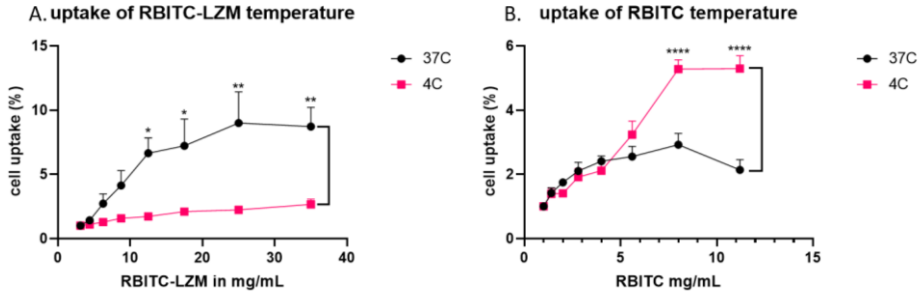

Figure 18. *Uptake of RBITC-LZM (A) and RBITC (B) in senescent ciPTEC-OAT1 after incubation at 4℃ or 37℃ for 3 hours.* Medium with RBITC or RBITC-LZM was introduced to the cells in a range of 0-11.2 mg/mL and 0-35 mg/mL respectively.

To further investigate that uptake of RBITC-LZM is based on LZM an inhibition assay was performed, results are shown in Figure 19.

A very slight decrease in RBITC-LZM uptake in senescent ciPTECs can be seen in the 1.62-4.87 mM LZM range but after the free LZM concentration increased to 6.50 and 8.12 mM (1:8 and 1:10, RBITC-LZM:LZM) a clear decrease in intake was observed. From 6.50 mM on, LZM concentrations are high enough that RBITC-LZM is inhibited. RB uptake is not impacted by LZM concentrations at any point.

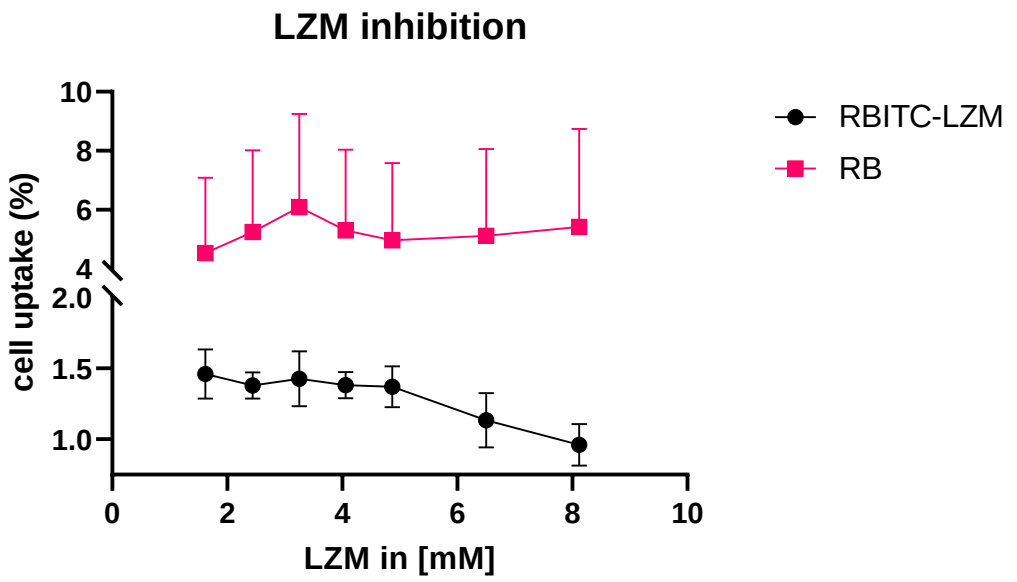

Figure 19. *Uptake of RBITC-LZM and Rhodamine B in senescent ciPTEC-OAT1 when inhibited with LZM.* Cells were incubated with 12.5 mg/mL LZM-RBITC or 2 mg/mL RB and excess LZM (1.62-8.12 mM) for 3h at 37°C.

4. Discussion & Conclusions

In this study, we examined a method to conjugate navitoclax to LZM through a three-step conjugation process. Second, we studied the suitability of ciPTEC-OAT1 as a model to study LZM-meditated drug delivery to the kidney.

Synthesis of the Senolytic-LZM conjugate

In this study, we attempt to use a platinum binder to connect a senolytic to LZM. Although this binder has been used before to bind a small molecule drug to LZM, to the extent of our knowledge this is the first time both bindings are attempted through an S-donor bond. The Lx binder can bind to ligands through its platinum center which can bind to two separate nucleophiles. Its binding affinity is based on Hard and Soft Acid and Base (HSAB) theory. Platinum as a soft acid has a preference to N-donor and S-donor ligands (Reedijk, 2012). Chloride ions are classified as a hard base, having low affinity for Pt and thus being a suitable leaving group for the reaction.

Many studies on the binding affinities of Pt are done using cisplatin. Cisplatin is a compound similar to Lx with two ammonia ligands instead of ethylenediamine and has been extensively researched due to its potency as an anti-cancer drug (Bugarčić et al., 2012). Its Pt center binds to N-donors on DNA, disrupting it and resulting in apoptosis (Dasari & Tchounwou, 2014). Affinity for binding is largely influenced by steric binding. Multiple binding sites are available on nucleic acids, but Lx strongly

prefers N7 on guanine. This is due to the steric interference on the other ligand sites when DNA is in its double-helix form (Reedijk, 2012).

When binding with an S-donor, Pt can bind to both thioether and thiol ligands. The Pt–S(thiol) bond is exceptionally stable and not easily displaced. However, when platinum binds to thioether ligands, the bond formation is faster but less stable compared to the Pt–S(thiol) bond. This difference in stability allows for the potential substitution of the sulfur atom in a Pt–S(thioether) bond by an N-bond (Bugarčić et al., 2012). However, in methionine binding Pt and methionine coordinate as a bidentate ligand forming a *S*,*N*-chelate. When methionine is added in excess to cisplatin, two methionine molecules bind to Pt in a chelated ring (Norman et al., 1992). The bond between navitoclax and Lx is a Pt-S(thioether) bond and not chelated although NMR should be performed to establish this.

As mentioned previously the novelty of the binding method of this study lies in using two S-donor bonds that binds both the drug and targeting protein to Lx. Lx has been used before in combination with LZM and has been linked through exposed methionine ligands forming a chelated thioether S-bond (M. E. M. Dolman et al., 2012; M. (Emmy) M. Dolman et al., 2012; Prakash et al., 2006, 2008). Furthermore, the linker has also been used to link to folate using an S-bond, this was done through a thiol bond on a hydrophilic spacer attached to folate (Shi et al., 2018). All these studies link the drug to Lx using the thermodynamically more stable and kinetically inert N-bond and then using an S-bond to link the drug-Lx complex to methionine although some studies have chosen to use histidine to link the complex to a protein due to its stability (Merkul et al., 2019). Waalboer et al. studied the binding properties of Lx to both S-donor and N-donor ligands. The study shows Pt-S (thioether) is a stable bond between Lx and an S-ligand and was subsequently bound to trastuzumab through naturally occurring amino acids. The Lx complex could have been bound through either methionine (thioether S-bond), cysteine (thiol S-bond) or histidine (N-bond). They added a thiourea quenching step to ensure the complex was bound using the more stable thiol S-bond and N-bond. Due to the quenching step, the bond between Lx and the ligand was broken (Waalboer et al., 2015). Although the S-bond between a small molecule and Lx was achieved, the study shows no data on the possibility of Lx using two thioether bonds as is attempted in this study.

Lx was able to bind to navitoclax and had the best binding results when reacted at room temperature for 3 days in a 5:1 (Lx: navitoclax) molar excess, see supplementary figure 3. When the reaction was done at 60℃, fragmentation of navitoclax was observed (Fig. S3A). As the binding of navitoclax to Lx is kinetically dependent (Waalboer et al., 2015), lowering the temperature to prevent fragmentation had no other effect on binding efficacy. Using the method described in this paper led to the binding of navitoclax with Lx with minimal fragmentation. Furthermore, the compound was stable enough to purify through preparative HPLC to a purity of 60-75%. In this study, no analysis was performed to study the resulting compounds for unbound Lx after filtration and preparative HPLC. Lx has a high cytotoxicity so no unbound Lx must be present in the final product. This can be tested using size exclusion UPLC with an MS detector.

In the three-step plan to synthesize navitoclax to LZM, the first two steps were successfully achieved. Navitoclax was bound to Lx and LZM was modified with exposed methionine residues. Navitoclax was bound 1:1 and up to four methionine molecules could be bound to one LZM, enabling higher drug-loading potential of the protein (Haselberg et al., 2011). LZM has seven possible binding sites in the form of six lysine residues and its N-terminus. This allows for 1099 methionine-LZM stoichiometries. In later steps, when the linking of navitoclax to the methionine residues is successful, a quantitative conjugate profile should be prepared to evaluate the drug-loading capabilities of the complex. The last step, binding of nav-Lx to LZM-m, was not successful. LZM-m was successfully bound to Lissamine-Lx, lissamine is bound to Lx through a spacer and an N-bond, and LZM-m was also

successfully bound to activated Lx, so we observed no problems with the exposure of methionine residues. We could attempt to bind Nav-Lx to methionine, this would exclude the possibility that LZM interferes with the binding of methionine residues to nav-Lx. The spacer could also be a factor in successful conjugation between LZM-m and Lissamine-Lx but failed binding of Nav-Lx to LZM-m. It is possible the binding site on Lx experiences steric shielding which is mitigated by the spacer. The spacer also increases solubility of the Lx-complex. Although the linker has made navitoclax more hydrophilic, it still needs DMF to dissolve. A high DMF content could denature LZM (Fujita & Noda, 1983) but it would be possible to increase DMF in a reaction between nav-Lx and methionine. If outcomes are different when the reaction is done in more DMF, nav-Lx could be modified using a spacer to increase solubility (Shi et al., 2018; Waalboer et al., 2015).

However, it is most likely that two S-bonds on one Pt linker is the problem in not achieving the final conjugation step. As two S-donor bonds on Lx has not been reported before, it could be that it is not possible due to steric interference. It has been reported before that Pt binding affinity is highly influenced by steric interference (Reedijk, 2012; Waalboer et al., 2015). This destabilization would also explain the slight increase in free navitoclax. In this case, it might be best to redirect so the linker uses one S-bond and one N-bond. LZM, which is now modified with methionine could be modified using a different amino acid that could form an N-bond with Lx. Boc-L-histidine N-hydroxysuccinimide ester could be bound to LZM using the same method as described in this paper and would be able to bond with Lx using an N-donor bond forming potential complex 1 (Fig. 20).

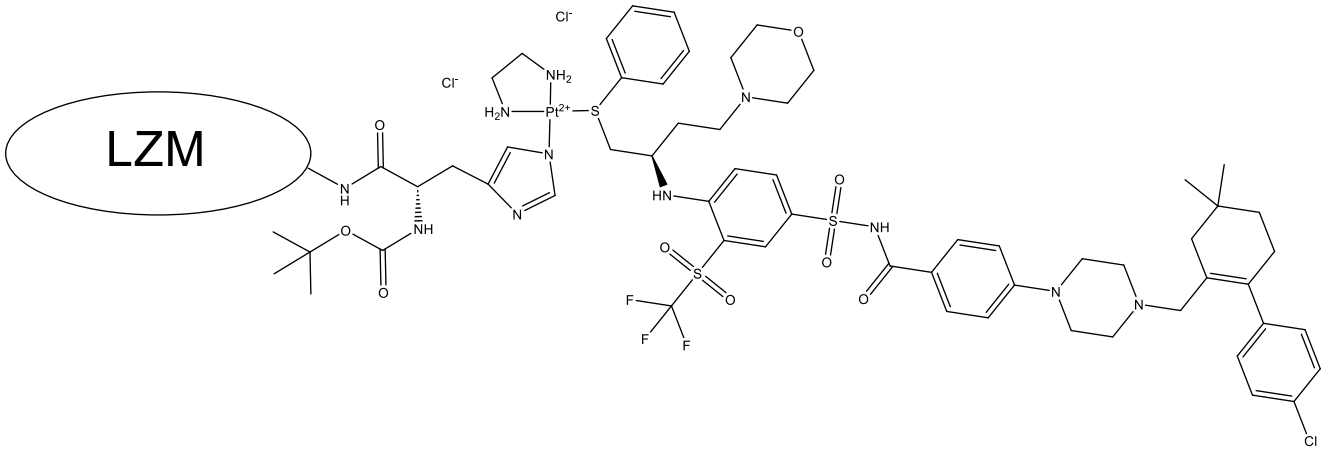

Figure 20. *Potential complex 1.* Navitoclax bound to Lx through an S-bond with Lx bound to LZM through an N-bond on a histidine residue.

It could also prove to be interesting to change the way navitoclax is bound to Lx. Next to the thioether that is used to bind to Lx in this study, there is another potential coordination site. The secondary amine next to the benzene could be used to bind to Lx. This bond would be more stable as compared to the thioether that is used in this study, but it would be quite difficult to achieve binding. The dissociation assay showed that all navitoclax was bound through an S-bond so the method discussed in this paper would not work. Another method that would allow for the conjugation of navitoclax to Lx through an N-bond is by creating a new binding site. The synthesis of navitoclax could be changed to create a binding site for Lx to bind through an N-bond (He et al., 2020). During synthesis Its morpholine ring needs to be replaced with a piperazine ring, creating a new binding site. This potential complex is shown in Figure 21 as potential complex 2. Forming an N-bond is

thermodynamically controlled (Waalboer et al., 2015) so the reaction method should take place at a high temperature. However, results show that performing the reaction at 60℃ leads to fragmentation of navitoclax. This leads us to believe that it would be more advantageous to change the senolytic to one that could form an N-bond with Lx or investigate other linkers.

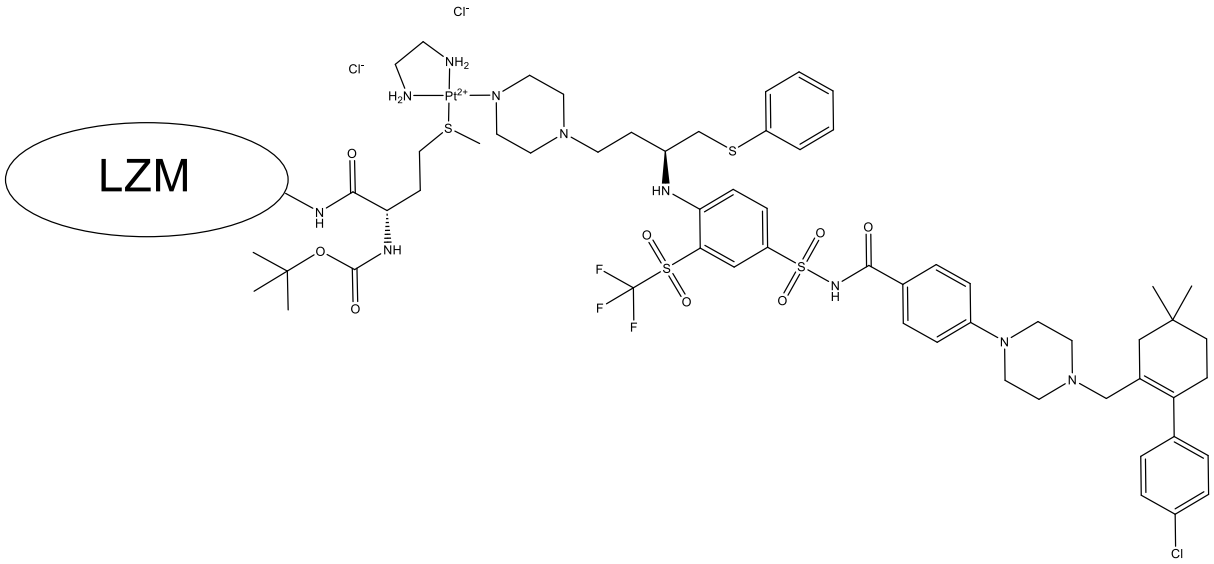

Figure 21. *Potential complex 2.* Altered navitoclax bound to Lx through an N-bond with Lx bound to LZM through a methionine residue.

The linking method between Navitoclax and LZM could be replaced. Galactose can be used as a linker molecule between navitoclax and LZM (Fig. 22). The previously mentioned secondary amine group can be used to bind to galactose (González-Gualda et al., 2020). Galactose can be modified using a succinimide or amine-activated reagent so it can bind to the lysine residues in LZM. Following receptor-mediated uptake, lysozyme allows for hydrolysis of galactose releasing navitoclax in the cell.

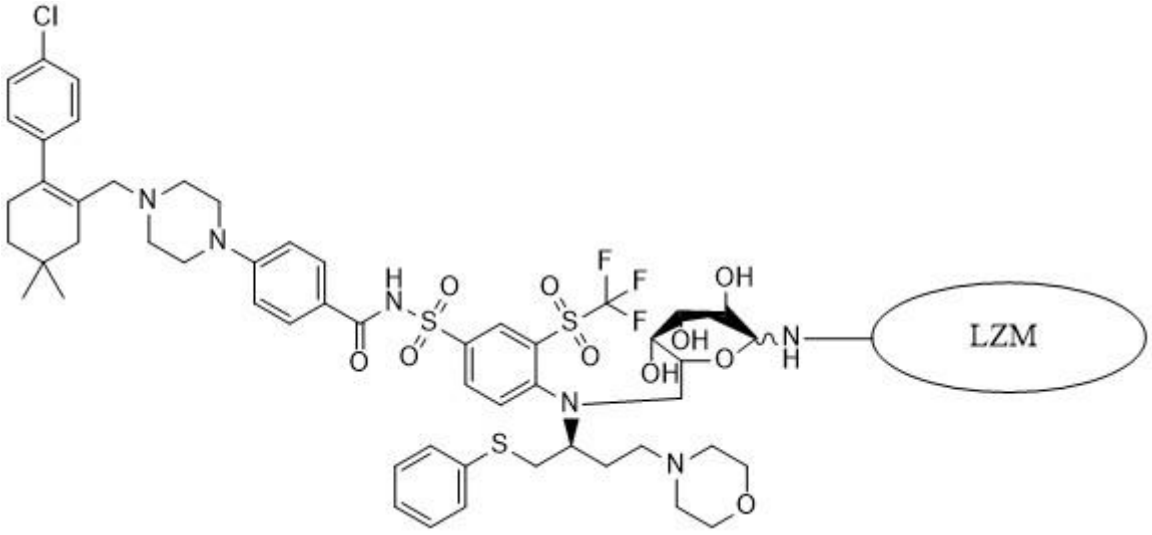

Figure 22. *Potential complex 3.* Navitoclax bound to LZM through a galactose linker.

Another method of conjugating navitoclax to LZM is through its morpholine ring. To use this method a slight change needs to be made when synthesizing navitoclax, the morpholine ring needs to be replaced with a piperazine ring. He et al. used this method to bind to 4-azidobutanoic acid, which can then be bound to a linker (He et al., 2020). The amine on the linker can conjugate to LZM and the triple-bound carbon will react with 4-azidobutanoic acid to form a triazole ring. The proposed complex is shown in Figure 23. To adapt this method for a drug delivery method, the degradability of the complex during cellular uptake should be studied to see if the degrading abilities of the lysosomes could break the bond between the piperazine ring and 4-azidobutanoic acid or if the degradation of the complex is solely dependent on LZM degradation. The efficacy of the leftover complex should be evaluated as well. The study showed that adapted navitoclax with the linker still had good binding with Bcl-XL but not with other members of the Bcl-2 family (He et al., 2020). Although the specificity of Bcl-XL alone should be enough to reach senolytic effects, its toxicity in senescent cells should be carefully evaluated.

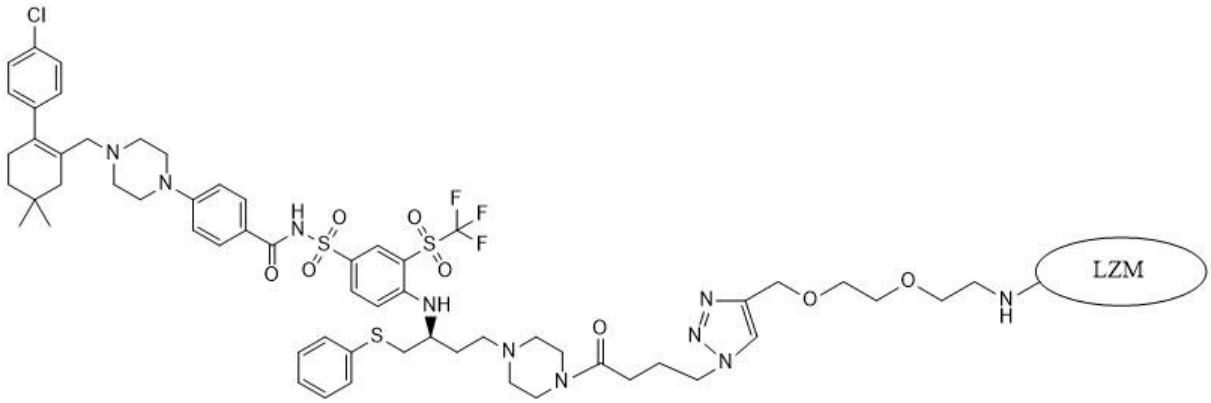

Figure 23. *Potential complex 4.* Altered navitoclax bound to LZM through an acid-linker process.

In conclusion, although a stable bond was formed between Lx and navitoclax, the final conjugation step was not successful. We propose some alternative strategies such as using a combination of S- and N-bonds or linker substitutions to overcome the limitations encountered in this study. Further investigation into these alternative strategies could pave the way to discovering a LZM-based targeted delivery method of a senolytic to senescent kidney cells.

RBITC-LZM to Study LZM Mediated Uptake in ciPTEC

Uptake of RBITC-LZM in ciPTECs presented as dose-dependent but not time-dependent. Although an incubation time of 3 hours increased uptake as compared to an incubation time of 1 hour, prolonging the incubation time to 6 hours resulted in no significant increase in fluorescence intensity (Fig. 17). Rapid uptake of RBITC-LZM is consistent with literature as in vivo experiments using drug-Lx-LZM have shown rapid accumulation of the conjugate in the kidney (Prakash et al., 2008). A plateau was reached 5 hours after injection. Intensity can also be decreased due to the exit of RBITC from the cell. RBITC, like other small molecules, can be exported from the cells through transporter protein P-gp (Altenberg et al., 1994; Sharom, 2011). Lastly, it is also possible that RBITC is metabolized into non-fluorescent compounds, decreasing the overall fluorescence.

When RBITC-LZM uptake in ciPTEC-OAT1 is compared to the uptake of RBITC, a big difference is observed. Longer incubation times lead to less uptake which could also be explained by free RBITC being able to leave the cell through transporter proteins. In the temperature assay, we observe a significant difference in uptake depending on temperature. Low uptake at a low temperature indicates that uptake is receptor-mediated as the endocytosis rate is extremely limited below a threshold of 10 ℃ (Weigel & Oka, 1981). RBITC uptake was not limited by lower temperatures, but increased uptake was observed. The cell membrane integrity could have been compromised due to the low temperatures, allowing RBITC to pass through passive diffusion. This would be consistent with the further observation that significantly higher uptake is observed at higher concentrations.

The effect of temperature and incubation time on the uptake of RBITC-LZM as compared to RBITC showed very different outcomes, which makes us conclude that the uptake of both compounds is regulated by different mechanisms which is consistent with our expectations. Furthermore, the LZM inhibition assay showed reduced uptake in RBITC-LZM when ciPTEC-OAT1were exposed to high concentrations of LZM while no change is seen in rhodamine B uptake. This indicates that the uptake of RBITC-LZM by ciPTEC-OAT1 is LZM mediated.

From these findings, we cannot yet conclude that the uptake of RBITC-LZM is megalin-dependent. To rule out that another form of entry that is LZM dependent is in play, we could compare ciPTEC-OAT1 to a megalin deficient cell line or ciPTEC-OAT1 with a megalin gene knock-out. Another way of confirming megalin-mediated uptake would be by further experiments with megalin inhibitors such as bradykinin or cilastatin (Alves et al., 2021; Hori et al., 2017) or competitive inhibition through megalin-exclusive ligands such as prolactin or RAP (Christensen & Birn, 2001; De et al., 2014).

Although RBITC-LZM was used to study the uptake of an LZM-small molecule complex in senescent ciPTEC, it cannot be used to study intracellular degradation of a drug-Lx-LZM complex. Prakash et al. showed that Rhodamine-Lx was still detected in vesicles in mice 24 hours after the first injection with a Rhodamine-Lx-LZM complex (Prakash et al., 2008). At this time point all carrier LZM had already been degraded, concluding that rhodamine-Lx was slowly degraded and released from lysosomes. This is further supported by Dolman et al. who showed that a drug-Lx-LZM conjugate is rapidly eliminated from the plasma but has slow renal accumulation of over 2 days (Dolman, 2012). Due to the effect Lx has on intracellular conjugate release, RBITC-LZM can only be used to study LZM-dependent uptake. Lissamine-Lx-m-LZM can be used to further study uptake and intracellular degradation and release of the conjugate to predict the pharmacokinetic parameters of a senolytic-Lx-LZM conjugate. Although the parameters might differ slightly as Lissamine and Lx are coupled through an N-bond and not an S-bond, as with Nav-Lx. Due to this less stable S-bond, the release might be faster as compared to other drug-Lx conjugates. Nevertheless, due to the conjugation of navitoclax with Lx a longer incubation time before performing a cell viability assay is needed to study this compound in vitro.

Furthermore, an increase in incubation time is also necessary to reach an effective dose. The highest concentration of RBITC-LZM tested was 35 mg/mL (2.4 mM). At this concentration, cellular uptake was at 16.6% for an incubation time of 3h (Fig. 17). Literature shows drug-Lx to LZM coupling ratio at 0.8:1, 1:1 and 1.2:1 (M. E. M. Dolman et al., 2012; Prakash et al., 2006, 2008). If conjugation of navitoclax to LZM was achieved in a 1:1 ratio, uptake would be at 0.4 mM. In vitro testing of the effect of navitoclax on senescent ciPTEC shows the LC50 of navitoclax is set at approximately 1 mM (Fig. 15), suggesting LZM uptake needs to be increased to reach the LC50 of a navitoclax-LZM conjugate. Cells showed little increase in RBITC-LZM uptake when the dose was heightened (an increase of 1.6% between 25 mg/mL to 35 mg/mL) or when the incubation time was prolonged to 6h (18.9% uptake). The low uptake increase when the dose was increased is probably due to the saturation of megalin

receptors, although the increased incubation time should have resolved this as megalin receptors get recycled back to the cell surface after endocytosis (Fig. 16). When the experiment was performed with free RBITC as a control, uptake decreased over time, indicating an efflux of RBITC. If free RBITC is leaving the cells the uptake at 6h of incubation would be higher than perceived. Increasing incubation time would allow for a higher uptake of a Nav-Lx-LZM conjugate to reach the LC50 of navitoclax in senescent ciPTEC.

The efflux of RBITC from the cells might indicate a problem that free navitoclax could also escape from the cells. However, Prakash et al. showed that after degradation of LZM, drug-Lx stays inside the cells and releases the drug in the environment (Prakash et al., 2006). Furthermore, in vivo results of drug-Lx-LZM studies report no free drug was found in the body after conjugate administration (M. E. M. Dolman et al., 2012; Prakash et al., 2006, 2008). To establish that no free drug can exit the cells, supernatant can be investigated for Nav-Lx and navitoclax using UPLC-UV.

In vitro results show RBITC-LZM uptake in ciPTEC-OAT1 is LZM-regulated endocytosis**.** We have established ciPTEC-OAT1 can be used as a suitable cell model to test LZM-mediated targeted delivery conjugates. Moreover, as navitoclax has shown a senolytic effect in senescence-like ciPTEC-OAT1 but no effect on non-senescent ciPTEC, we believe the model is also suitable for senolytic-LZM conjugates. Further research using megalin knock-out approaches could confirm these findings. To study release of the drug in the cytosol an Lx containing conjugate such as Lissamine-Lx-m-LZM should be used to account for the effect Lx has on lysosomal release within the cells.

References

Altenberg, G. A., Vanoye, C. G., Han, E. S., Deitmer, J. W., & Reuss, L. (1994). Relationships between rhodamine 123 transport, cell volume, and ion-channel function of P-glycoprotein. *The Journal of Biological Chemistry*, *269*(10), 7145–7149.

Alves, S. A. S., Florentino, L. S., Teixeira, D. E., Silva-Aguiar, R. P., Peruchetti, D. B., Oliveira, A. C., Scharfstein, J., Marzolo, M.-P., Pinheiro, A. A. S., & Caruso-Neves, C. (2021). Surface megalin expression is a target to the inhibitory effect of bradykinin on the renal albumin endocytosis. *Peptides*, *146*, 170646. https://doi.org/10.1016/j.peptides.2021.170646

Bugarčić, Ž. D., Bogojeski, J., Petrović, B., Hochreuther, S., & Eldik, R. van. (2012). Mechanistic studies on the reactions of platinum(II) complexes with nitrogen- and sulfur-donor biomolecules. *Dalton Transactions*, *41*(40), 12329–12345. https://doi.org/10.1039/C2DT31045G

Caetano-Pinto, P., Janssen, M. J., Gijzen, L., Verscheijden, L., Wilmer, M. J. G., & Masereeuw, R. (2016). Fluorescence-Based Transport Assays Revisited in a Human Renal Proximal Tubule Cell Line. *Molecular Pharmaceutics*, *13*(3), 933–944. https://doi.org/10.1021/acs.molpharmaceut.5b00821

Chaib, S., Tchkonia, T., & Kirkland, J. L. (2022). Cellular senescence and senolytics: The path to the clinic. *Nature Medicine*, *28*(8), Article 8. https://doi.org/10.1038/s41591-022-01923-y

Chen, T. K., Knicely, D. H., & Grams, M. E. (2019). Chronic Kidney Disease Diagnosis and Management. *JAMA*, *322*(13), 1294–1304. https://doi.org/10.1001/jama.2019.14745

Christensen, E. I., & Birn, H. (2001). Megalin and cubilin: Synergistic endocytic receptors in renal proximal tubule. *American Journal of Physiology-Renal Physiology*, *280*(4), F562–F573. https://doi.org/10.1152/ajprenal.2001.280.4.F562

Chronic kidney disease—Treatment. (2017, October 20). Nhs.Uk. https://www.nhs.uk/conditions/kidney-disease/treatment/

Coppé, J.-P., Desprez, P.-Y., Krtolica, A., & Campisi, J. (2010). The Senescence-Associated Secretory Phenotype: The Dark Side of Tumor Suppression. *Annual Review of Pathology*, *5*, 99–118. https://doi.org/10.1146/annurev-pathol-121808-102144

Dai, L., Qureshi, A. R., Witasp, A., Lindholm, B., & Stenvinkel, P. (2019). Early Vascular Ageing and Cellular Senescence in Chronic Kidney Disease. *Computational and Structural Biotechnology Journal*, *17*, 721–729. https://doi.org/10.1016/j.csbj.2019.06.015

Dasari, S., & Tchounwou, P. B. (2014). Cisplatin in cancer therapy: Molecular mechanisms of action. *European Journal of Pharmacology*, *740*, 364–378. https://doi.org/10.1016/j.ejphar.2014.07.025

De, S., Kuwahara, S., & Saito, A. (2014). The Endocytic Receptor Megalin and its Associated Proteins in Proximal Tubule Epithelial Cells. *Membranes*, *4*(3), 333–355. https://doi.org/10.3390/membranes4030333

Docherty, M.-H., O'Sullivan, E. D., Bonventre, J. V., & Ferenbach, D. A. (2019). Cellular Senescence in the Kidney. *Journal of the American Society of Nephrology : JASN*, *30*(5), 726–736. https://doi.org/10.1681/ASN.2018121251

Dolman, M. E. M., van Dorenmalen, K. M. A., Pieters, E. H. E., Lacombe, M., Pato, J., Storm, G., Hennink, W. E., & Kok, R. J. (2012). Imatinib-ULS-lysozyme: A proximal tubular cell-targeted conjugate of imatinib for the treatment of renal diseases. *Journal of Controlled Release: Official Journal of the Controlled Release Society*, *157*(3), 461–468. https://doi.org/10.1016/j.jconrel.2011.08.041

Dolman, M. (Emmy) M., Harmsen, S., Pieters, E. H., Sparidans, R. W., Lacombe, M., Szokol, B., Őrfi, L., Kéri, G., Storm, G., Hennink, W. E., & Kok, R. J. (2012). Targeting of a platinum-bound sunitinib analog to renal proximal tubular cells. *International Journal of Nanomedicine*, *7*, 417–433. https://doi.org/10.2147/IJN.S26485

Fujita, Y., & Noda, Y. (1983). The Effect of Organic Solvents on the Thermal Denaturation of Lysozyme as Measured by Differential Scanning Calorimetry. *Bulletin of the Chemical Society of Japan*, *56*(1), 233–237. https://doi.org/10.1246/bcsj.56.233

González-Gualda, E., Pàez-Ribes, M., Lozano-Torres, B., Macias, D., Wilson, J. R., González-López, C., Ou, H.-L., Mirón-Barroso, S., Zhang, Z., Lérida-Viso, A., Blandez, J. F., Bernardos, A., Sancenón, F., Rovira, M., Fruk, L., Martins, C. P., Serrano, M., Doherty, G. J., Martínez-Máñez, R., & Muñoz-Espín, D. (2020). Galacto-conjugation of Navitoclax as an efficient strategy to increase senolytic specificity and reduce platelet toxicity. *Aging Cell*, *19*(4), e13142. https://doi.org/10.1111/acel.13142

Haas, M., Kluppel, A. C. A., Wartna, E. S., Moolenaar, F., Meijer, D. K. F., De Jong, P. E., & De Zeeuw, D. (1997). Drug-targeting to the kidney: Renal delivery and degradation of a naproxen-lysozyme conjugate in vivo. *Kidney International*, *52*(6), 1693–1699. https://doi.org/10.1038/ki.1997.504

Haselberg, R., Harmsen, S., Dolman, M. E. M., de Jong, G. J., Kok, R. J., & Somsen, G. W. (2011). Characterization of drug-lysozyme conjugates by sheathless capillary electrophoresis–time-of-flight mass spectrometry. *Analytica Chimica Acta*, *698*(1), 77–83. https://doi.org/10.1016/j.aca.2011.04.050

He, Y., Zhang, X., Chang, J., Kim, H.-N., Zhang, P., Wang, Y., Khan, S., Liu, X., Zhang, X., Lv, D., Song, L., Li, W., Thummuri, D., Yuan, Y., Wiegand, J. S., Ortiz, Y. T., Budamagunta, V., Elisseeff, J. H., Campisi, J., … Zhou, D. (2020). Using proteolysis-targeting chimera technology to reduce navitoclax platelet toxicity and improve its senolytic activity. *Nature Communications*, *11*(1), Article 1. https://doi.org/10.1038/s41467-020-15838-0

Hill, N. R., Fatoba, S. T., Oke, J. L., Hirst, J. A., O'Callaghan, C. A., Lasserson, D. S., & Hobbs, F. D. R. (2016). Global Prevalence of Chronic Kidney Disease – A Systematic Review and Meta-Analysis. *PLoS ONE*, *11*(7), e0158765. https://doi.org/10.1371/journal.pone.0158765

Hori, Y., Aoki, N., Kuwahara, S., Hosojima, M., Kaseda, R., Goto, S., Iida, T., De, S., Kabasawa, H., Kaneko, R., Aoki, H., Tanabe, Y., Kagamu, H., Narita, I., Kikuchi, T., & Saito, A. (2017). Megalin Blockade with Cilastatin Suppresses Drug-Induced Nephrotoxicity. *Journal of the American Society of Nephrology: JASN*, *28*(6), 1783–1791. https://doi.org/10.1681/ASN.2016060606

Kirkland, J. L., & Tchkonia, T. (2020). Senolytic drugs: From discovery to translation. *Journal of Internal Medicine*, *288*(5), 518. https://doi.org/10.1111/joim.13141

Kok, R. J., Haas, M., Moolenaar, F., de Zeeuw, D., & Meijer, D. K. F. (1998). Drug Delivery to the Kidneys and the Bladder with the Low Molecular Weight Protein Lysozyme. *Renal Failure*, *20*(2), 211–217. https://doi.org/10.3109/08860229809045104

Kovesdy, C. P. (2022). Epidemiology of chronic kidney disease: An update 2022. *Kidney International Supplements*, *12*(1), 7–11. https://doi.org/10.1016/j.kisu.2021.11.003

Melk, A., Schmidt, B. M. W., Vongwiwatana, A., Rayner, D. C., & Halloran, P. F. (2005). Increased expression of senescence-associated cell cycle inhibitor p16INK4a in deteriorating renal transplants and diseased native kidney. *American Journal of Transplantation: Official Journal of the American Society of Transplantation and the American Society of Transplant Surgeons*, *5*(6), 1375–1382. https://doi.org/10.1111/j.1600-6143.2005.00846.x

Merkul, E., Sijbrandi, N. J., Muns, J. A., Aydin, I., Adamzek, K., Houthoff, H.-J., Nijmeijer, B., & Van Dongen, G. A. M. S. (2019). First platinum(II)-based metal-organic linker technology (Lx®) for a plug-and-play development of antibody-drug conjugates (ADCs). *Expert Opinion on Drug Delivery*, *16*(8), 783–793. https://doi.org/10.1080/17425247.2019.1645118

Metzger, M., Abdel-Rahman, E. M., Boykin, H., & Song, M.-K. (2021). A Narrative Review of Management Strategies for Common Symptoms in Advanced CKD. *Kidney International Reports*, *6*(4), 894–904. https://doi.org/10.1016/j.ekir.2021.01.038

Moranne, O., Froissart, M., Rossert, J., Gauci, C., Boffa, J.-J., Haymann, J. P., M'rad, M. B., Jacquot, C., Houillier, P., Stengel, B., & Fouqueray, B. (2009). Timing of Onset of CKD-Related Metabolic

Complications. *Journal of the American Society of Nephrology : JASN*, *20*(1), 164–171. https://doi.org/10.1681/ASN.2008020159

Norman, R. E., Ranford, J. D., & Sadler, P. J. (1992). Studies of platinum(II) methionine complexes: Metabolites of cisplatin. *Inorganic Chemistry*, *31*(5), 877–888. https://doi.org/10.1021/ic00031a033

Prakash, J., de Borst, M. H., van Loenen-Weemaes, A. M., Lacombe, M., Opdam, F., van Goor, H., Meijer, D. K. F., Moolenaar, F., Poelstra, K., & Kok, R. J. (2008). Cell-specific Delivery of a Transforming Growth Factor-beta Type I Receptor Kinase Inhibitor to Proximal Tubular Cells for the Treatment of Renal Fibrosis. *Pharmaceutical Research*, *25*(10), 2427–2439. https://doi.org/10.1007/s11095-007-9515-x

Prakash, J., Sandovici, M., Saluja, V., Lacombe, M., Schaapveld, R. Q. J., Borst, M. H. de, Goor, H. van, Henning, R. H., Proost, J. H., Moolenaar, F., Këri, G., Meijer, D. K. F., Poelstra, K., & Kok, R. J. (2006). Intracellular Delivery of the p38 Mitogen-Activated Protein Kinase Inhibitor SB202190 [4-(4-Fluorophenyl)-2-(4-hydroxyphenyl)-5-(4-pyridyl)1H-imidazole] in Renal Tubular Cells: A Novel Strategy to Treat Renal Fibrosis. *Journal of Pharmacology and Experimental Therapeutics*, *319*(1), 8–19. https://doi.org/10.1124/jpet.106.106054

Reedijk, J. (2012). Fast and slow versus strong and weak metal–DNA binding: Consequences for anti-cancer activity. *Metallomics*, *4*(7), 628–632. https://doi.org/10.1039/c2mt20032e

Rizzo, R., Onesto, V., Forciniti, S., Chandra, A., Prasad, S., Iuele, H., Colella, F., Gigli, G., & del Mercato, L. L. (2022). A pH-sensor scaffold for mapping spatiotemporal gradients in three-dimensional in vitro tumour models. *Biosensors and Bioelectronics*, *212*, 114401. https://doi.org/10.1016/j.bios.2022.114401

Schroth, J., Thiemermann, C., & Henson, S. M. (2020). Senescence and the Aging Immune System as Major Drivers of Chronic Kidney Disease. *Frontiers in Cell and Developmental Biology*, *8*, 564461. https://doi.org/10.3389/fcell.2020.564461

Sharom, F. J. (2011). The P-glycoprotein multidrug transporter. *Essays in Biochemistry*, *50*(1), 161–178. https://doi.org/10.1042/bse0500161

Shi, H., Leonhard, W., Sijbrandi, N., Van Steenbergen, M., Fens, M., Van den Dikkenberg, J., Toraño, J., Peters, D., Hennink, W., & Kok, R. (2018). Folate-dactolisib conjugates for targeting tubular cells in polycystic kidneys. *Journal of Controlled Release*, *293*. https://doi.org/10.1016/j.jconrel.2018.11.019

Sturmlechner, I., Durik, M., Sieben, C. J., Baker, D. J., & van Deursen, J. M. (2017). Cellular senescence in renal ageing and disease. *Nature Reviews. Nephrology*, *13*(2), 77–89. https://doi.org/10.1038/nrneph.2016.183

Sun, Y., Goes Martini, A., Janssen, M. J., Garrelds, I. M., Masereeuw, R., Lu, X., & Danser, A. H. J. (2020). Megalin: A Novel Endocytic Receptor for Prorenin and Renin. *Hypertension (Dallas, Tex.: 1979)*, *75*(5), 1242–1250. https://doi.org/10.1161/HYPERTENSIONAHA.120.14845

Waalboer, D. C. J., Muns, J. A., Sijbrandi, N. J., Schasfoort, R. B. M., Haselberg, R., Somsen, G. W., Houthoff, H.-J., & van Dongen, G. A. M. S. (2015). Platinum(II) as Bifunctional Linker in Antibody–Drug Conjugate Formation: Coupling of a 4-Nitrobenzo-2-oxa-1,3-diazole Fluorophore to Trastuzumab as a Model. *ChemMedChem*, *10*(5), 797–803. https://doi.org/10.1002/cmdc.201402496

Wang, Y., Sun, Y., Wang, H., Liu, P., Peng, W., & Duan, Y. (2013). Synthesis of low-molecular weight protein (LMWP) lysozyme–curcumin conjugates for kidney drug targeting. *Journal of Biomaterials Science, Polymer Edition*, *24*(11), 1360–1367. https://doi.org/10.1080/09205063.2012.759506

Weigel, P. H., & Oka, J. A. (1981). Temperature dependence of endocytosis mediated by the asialoglycoprotein receptor in isolated rat hepatocytes. Evidence for two potentially rate-limiting steps. *Journal of Biological Chemistry*, *256*(6), 2615–2617. https://doi.org/10.1016/S0021-9258(19)69656-0

Wilmer, M. J., Saleem, M. A., Masereeuw, R., Ni, L., van der Velden, T. J., Russel, F. G., Mathieson, P. W., Monnens, L. A., van den Heuvel, L. P., & Levtchenko, E. N. (2010). Novel conditionally immortalized human proximal tubule cell line expressing functional influx and efflux transporters. *Cell and Tissue Research*, *339*(2), 449–457. https://doi.org/10.1007/s00441-009-0882-y

Wilson, J. J., & Lippard, S. J. (2014). Synthetic Methods for the Preparation of Platinum Anticancer Complexes. *Chemical Reviews*, *114*(8), 4470–4495. https://doi.org/10.1021/cr4004314

Wilson, W. H., O'Connor, O. A., Czuczman, M. S., LaCasce, A. S., Gerecitano, J. F., Leonard, J. P., Tulpule, A., Dunleavy, K., Xiong, H., Chiu, Y.-L., Cui, Y., Busman, T., Elmore, S. W., Rosenberg, S. H., Krivoshik, A. P., Enschede, S. H., & Humerickhouse, R. A. (2010). Navitoclax, a targeted high-affinity inhibitor of BCL-2, in lymphoid malignancies: A phase 1 dose-escalation study of safety, pharmacokinetics, pharmacodynamics, and antitumour activity. *The Lancet Oncology*, *11*(12), 1149–1159. https://doi.org/10.1016/S1470-2045(10)70261-8

Yang, Y., Mihajlovic, M., Valentijn, F., Nguyen, T. Q., Goldschmeding, R., & Masereeuw, R. (2022). A Human Conditionally Immortalized Proximal Tubule Epithelial Cell Line as a Novel Model for Studying Senescence and Response to Senolytics. *Frontiers in Pharmacology*, *13*. https://www.frontiersin.org/articles/10.3389/fphar.2022.791612

Zhang, Z., Zheng, Q., Han, J., Gao, G., Liu, J., Gong, T., Gu, Z., Huang, Y., Sun, X., & He, Q. (2009). The targeting of 14-succinate triptolide-lysozyme conjugate to proximal renal tubular epithelial cells. *Biomaterials*, *30*(7), 1372–1381. https://doi.org/10.1016/j.biomaterials.2008.11.035

Zhao, J.-L., Qiao, X.-H., Mao, J.-H., Liu, F., & Fu, H.-D. (2022). The interaction between cellular senescence and chronic kidney disease as a therapeutic opportunity. *Frontiers in Pharmacology*, *13*, 974361. https://doi.org/10.3389/fphar.2022.974361

Zheng, Q., Gong, T., Sun, X., & Zhang, Z.-R. (2006). Synthesis, characterization andin vitro evaluation of triptolide-lysozyme conjugate for renal targeting delivery of triptolide. *Archives of Pharmacal Research*, *29*(12), 1164–1170. https://doi.org/10.1007/BF02969309